DOI: 10.26599/FSHW.2026.9251083

Contents lists available at SciOpen

Food Science and Human Wellness

journal homepage: https://www.sciopen.com/journal/2097-0765

China Food Publishing Co.

Preparation of N,O-carboxymethyl chitosan-iron complex and its effect on improving brain cognitive function of offspring through mother-to-infant microbiota vertical transmission

Pan Liu, Mingrui Zhang, Tianyu Dong, Yingyue Cui, Huichen Yan, Haotian Wang, Xiaoxi Liu, Xinyi Feng, Yi Wu *

State Key Laboratory of Animal Nutrition and Feeding, College of Animal Science and Technology, China Agricultural University, Beijing 100193, China

ABSTRACT: Maternal iron deficiency is closely associated with cognitive deficits in offspring. Polysaccharide-iron complexes as iron supplements have the advantages of fewer gastrointestinal side effects and higher iron content. Furthermore, the polysaccharides themselves can sustain intestinal and metabolic health. N,O-carboxymethyl chitosan (N,O-CMCS) is an important derivative of chitosan with excellent water solubility, and it can chelate metal ions more effectively than chitosan. This study employed N,O-CMCS and ammonium ferrous sulfate to synthesize a novel N,O-CMCS-iron complex containing 35.96% iron. The structure of the complex was characterized by scanning electron microscope, Fourier transform infrared spectrometer and ultraviolet spectrophotometer. We then explored the impact of maternal N,O-CMCS-iron intake during pregnancy and lactation on iron status and cognitive function in offspring mice. The results showed that compared with the inorganic iron, maternal exposure to N,O-CMCS-iron significantly increased iron storage in dams and offspring, and improved the contents of neuroplasticity-related molecules as well as the behavioral performance, despite the offspring switched to a normal diet. Moreover, maternal consumption of N,O-CMCS-iron simultaneously regulated the gut microbiota composition of dams and offspring, enhancing the abundances of butyrate-producing bacteria like *Butyricimonas* and *Clostridium*, and elevated the butyrate level. Such sustained alterations in microbiota and butyrate were relevant to the enrichment of HIF-1α signaling in the offspring brain, which may be the reason for promoting physiological processes including angiogenesis, glucose metabolism, and iron uptake in the brain, and ultimately enhancing cognitive function. This study supports that the N,O-CMCS-iron complex markedly elevates the iron content, and that its ability to modulate the gut-brain connection contributes to its role in improving brain cognition.

Keywords: Iron deficiency; N,O-carboxymethyl chitosan-iron; cognitive function; gut microbiota; butyrate; HIF-1α signaling

1. Introduction

Iron deficiency has been a worldwide problem of epidemic proportions, which principally affects woman and children not just in low- and middle-income nations but even in developed nations[1]. As one of the most significant minerals in body, iron is essential for several physiological functions, including oxygen

***Corresponding author**
wuyi2013@cau.edu.cn

Received 4 July 2025
Received in revised from 15 September 2025
Accepted 24 December 2025

transportation, cell repair, and DNA proliferation. And importantly, iron plays a key role in brain development since it is a critical factor for myelin production, dopamine function and neuronal metabolism[2].

Cognitive development is grounded in the formation and maturation of brain, a hypersensitive process that initiates at the fetal stage. The prenatal environment, especially the maternal nutritional status, is vital to the fetal brain development[3]. During pregnancy, the larger blood volume and growth of the fetus, placenta and other maternal tissues result in an increased demand for iron, making it important to ensure an sufficient supply of iron[4]. Despite the placenta has an active regulatory capacity for iron transport, maternal iron deficiency is linked to lower fetal iron reserves. It is reported that children with a worse iron status in the womb had significantly poorer verbal and fine motor capabilities[5]. An animal study using rats as models showed that prenatal and perinatal iron deficiency triggered cognitive and behavioral dysfunctions in offspring, and could not be corrected by early postnatal iron supplementation[6]. In addition, it has been noted that mothers who are iron deficient have a higher chance of their children developing schizophrenia[2]. The growing evidence suggests that maternal iron status has profound effects on the cognition and neurobehavior of offspring.

Iron salts are available iron supplements used for the management of iron deficiency, and ferrous sulfate is the most commonly used agent of all ages. However, some gastrointestinal adverse effects including nausea, abdominal pain and diarrhea have been reported upon long-term administration of ferrous sulfate[7]. Since pregnant women already suffer from vomiting and other physiological symptoms, the intake of ferrous sulfate might further aggravate the gastrointestinal discomfort. Therefore, in spite of the potential efficacy of ferrous iron, there is an obvious requirement for other iron supplements with fewer adverse effects. The polysaccharide-iron complex preparations have excellent stability as well as fewer side effects, making them one of the most recommended regents currently. And these complexes usually maintain relatively high concentrations of iron under physiological conditions[8,9]. What's more, polysaccharides themselves can also exert a variety of beneficial roles, which include hypoglycemic, anti-oxidant and intestinal microecological effects. Several polysaccharide-iron complexes have been utilized to treat iron deficiency, such as dextran-iron and sucrose-iron complexes[10,11].

There is a rising awareness that the gut microbiota holds a pivotal function in iron metabolism and brain development. According to reports, the gut microbiota modulates the expression of genes engaged in iron uptake and secretes cofactors that facilitate iron transport, making it crucial for intestinal and systemic iron homeostasis[12,13]. Germ-free mice had less iron stored in the spleen, kidney and liver compared to the control animals[12]. Furthermore, research showed that alterations in brain iron and cognitive function paralleled to changes in certain bacterial phyla in the intestine[14], indicating a possible association between gut microbes and brain iron availability. Notably, the intestinal microbiome forms a complex and bidirectional link with brain that can affect brain function and behavior. Imbalance of intestinal microecology is associated with various neurological disorders, including depression, anxiety, and

neurodegenerative diseases such as Alzheimer's[15]. The gut-brain axis is a key mechanism by which probiotics and prebiotics influence neurological and mental health conditions[16]. Mechanisms including vagus nerve communication, immunological regulation, and the synthesis of microbial metabolites and neurotransmitters facilitate this connection[17].

The colonization of gut microbiota may be affected by maternal symbiotic bacteria that are present in several parts of the mothers' body, such as the gut, birth canal and skin. The maternal gut microbiota is the most crucial source for infants' acquired strains, as the maternal gut microbial strains were more stable and long-lasting in the infant gut than microbes contributed by other sources[18]. The diet ingested by a host can modulate its gut microbiota and influence its metabolic phenotype. Thus, the maternal diet not only affects its own metabolism, but may also exert microbe-dependent effects on the metabolic phenotype of its offspring. A study revealed that maternal high-fat diet induced gut flora disruption, leading to impaired social behavior in mice offspring[19]. And another study demonstrated that the offspring mice of dams who underwent fiber deprivation during lactation had reduced intestinal diversity, causing low-grade inflammation and a tendency to obesity[20]. It can be seen that maintaining a healthy maternal gut microbiome benefits the offspring development.

Chitosan is a natural linear polysaccharide produced by deacetylation of chitin, which is the second most abundant polysaccharide in nature (after cellulose). Chitosan is structurally composed of β-(1-4)-linked N-acetyl-D-glucosamine and D-glucosamine. And the amino and hydroxyl groups on the chitosan backbone provide unique chelation sites for most metal ions. The exceptional properties of chitosan including non-toxicity, biocompatibility and biodegradability make it desirable for a wide range of applications[21]. In a small number of animal model studies, chitosan and its derivatives have shown positive impacts in intestinal microbiota alteration, and thus perform their advantageous biological functions. A study showed that the chitosan consumption lessened menopausal symptoms of rats by adjusting the gut microbiota composition and elevating the short-chain fatty acid level in feces[22]. Additionally, Lin et al. illustrated that chitosan oligosaccharides significantly prevented hindlimb ischemia in mice, which may be related to their improvement of intestinal bacterial structure and further regulation of plasma metabolite contents in mice[23]. It's worth noting that chitosan is prone to chemical modifications such as carboxymethyl methylation. The resulting carboxymethyl chitosan (CMCS) can not only improve the water solubility of chitosan but also enhance its original properties. Carboxymethylation can occur on the amino or hydroxyl groups of chitosan, and the corresponding products are mainly N-CMCS, O-CMCS, or N,O-CMCS. It is reported that CMCS has a stronger loading capacity for metal ions, and has been widely used in many fields such as food, medicine and agriculture[24].

Taken as a whole, it is very potential for the CMCS-iron complex to be exploited as a novel iron supplement which has a synergism on brain development. This study prepared and characterized the novel N,O-CMCS-iron complex, and investigated the effects of maternal intake of N,O-CMCS-iron during pregnancy and lactation on the iron level and cognitive function of the offspring mice by establishing a

maternal iron deficiency model. The present study would help develop a new-type efficient polysaccharide-iron supplement, and provide new insights into the mechanism by which maternal intake of N,O-CMCS-iron complex improves the brain cognitive function of offspring.

2. Materials and Methods

2.1. Ethical Statement

All animal experiments in this study were implemented in agreement with protocals approved by the Institutional Animal Care and Use Committee of China Agricultural University (permission code: AW31402202-1-3). All animal procedures complied with the National Research Council Guide for the Care and Use of Laboratory Animals.

2.2. Preparation of the N,O-CMCS-iron complex

N,O-CMCS was obtained from Aladdin Biochemical Technology Co., Ltd.. The N,O-CMCS-iron complex was synthesized based on a previous study[25]. Specifically, we dissolved 0.1g N,O-CMCS into 20 mL sodium acetate-acetic acid buffer solution (pH 5.6), and added 20 mL ammonium ferrous sulfate solution ($(NH4)_2SO_4 \cdot FeSO_4 \cdot 6H_2O$) with a concentration of 0.06 mol/L into it, next we stirred the solution at room temperature for 30 min. After the production of reddish-brown sediment, the solution was allowed to stand for 30 min. The precipitate was collected and washed with 70% ethanol and then washed with anhydrous ethanol several times until no Fe^{2+} could be detected. The final product was obtained as a reddish-brown powder after vacuum freeze-drying. The final iron content of the N,O-CMCS-iron complex was determined to be 35.96%.

2.3. Structural characterization of N,O-CMCS and the N,O-CMCS-iron complex

2.3.1. Determination of the degree of deacetylation (DD) and the degree of substitution (DS)

The DD and DS of N,O-CMCS were determined by potentiometric titration and the hydrogen nucleus magnetic resonance spectroscopy (^{1}H NMR). Briefly, 0.1 g N,O-CMCS was dissolved in 20 mL of hydrochloric acid (0.3mol/L) and titrated with 0.1mol/L sodium hydroxide. The pH was recorded with a calibrated pH-meter. Finally, the two parameters were calculated according to the following equations (eq. 1 and 2.):

$$\mathrm{DS} = \frac{203 \times \triangle V_1 \times c_1}{m \times (1 - w_0) - 80 \times \triangle V_1 \times c_1 + 42 \times \triangle V_2 \times c_1} \times 100\% \quad (1)$$

$$\mathrm{DD} = \frac{203 \times \triangle V_2 \times c_1}{m \times (1 - w_0) - 80 \times \triangle V_1 \times c_1 + 42 \times \triangle V_2 \times c_1} \times 100\% \quad (2)$$

where 203 is the relative molecular weight of the N-acetylamino-D-glucose; ΔV_1 is the difference in volume of NaOH consumed between the first and second inflection points (mL); ΔV_2 is the difference in volume of NaOH consumed between the third and second inflection points (mL); c_1 is the concentration of

NaOH (mol/L); m is the mass of the sample (mg); w_0 is the weight loss on drying of the sample (%); 80 is the relative molecular mass of sodium carboxymethyl; and 42 is the relative molecular mass of acetyl.

^{1}H NMR analysis was carried out with a Bruker Ascend 600 MHZ spectrometer (Bruker, Germany). The N,O-CMCS sample was dissolved in Dcl and placed in a 5 mm diameter tube. The parameters were set as follows: 600 MHz spectral window, 32 k data points, 45◦ pulse angle, and 32 scans. And finally the DD and DS of N,O-CMCS were measured[26,27].

2.3.2. Determination of molecular weight

The molecular weights of N,O-CMCS and the N,O-CMCS-iron complex were determined by high-performance gel-filtration chromatography (HPGFC) (Waters Alliance 2695, Waters, USA). Separation was achieved on a TSK-G3000 PWxL column (300 mm × 7.8 mm id) eluted with 0.1 M sodium acetate and 1% acetic acid. The flow rate was 0.5 mL/min and the column temperature was maintained at 40°C.

2.3.3. Structural analysis

The microstructures of N,O-CMCS and the N,O-CMCS-iron complex were observed by scanning electron microscope (SEM, Zeiss Gemini 360). Besides, Fourier transform infrared spectrometer (FT-IR spectrometer, Thermo Nicolet IS5/IS10) was used to obtain the spectra of N,O-CMCS and the N,O-CMCS-iron complex between 4000 and 400 cm^{-1}. In addition, N,O-CMCS and the N,O-CMCS-iron complex were dissolved in 0.1 mol/L hydrochloric acid solution respectively and detected on a ultraviolet spectrophotometer (UV-1600) with a wavelength scanning range of 200-800 nm.

2.4. Animal and experimental design

Specific pathogen-free (SPF) female ICR mice (SiPeiFu Biotechnology Co., LTD, Beijing, China) with an average weight of 22 g were used in the experiment. In Exp. 1, female mice were mated and conception was confirmed by the presence of a vaginal plug. After 0.5 days of vaginal plug, mice were split into three groups at random (n = 10): the low-dose ferrous sulfate group (LI), namely the iron deficiency group; the normal dose ferrous sulfate supplement group (NI); and the N,O-CMCS-iron supplement group (CI). Females in the LI group were fed a diet with less than 5 ppm iron provided by ferrous sulfate. For the NI group, females were fed a base diet of 45 ppm iron provided by ferrous sulfate. And in the CI group, females were fed a diet of 45 ppm iron provided by the N,O-CMCS-iron complex. The total gestation period was 21 days. Within 24 h of delivery, 20 pups were retained in each group (half male and half female). At the end of the 21-day lactation period, the dams and 10 offspring from each group were sacrificed. And the remaining 10 offspring from each group proceeded to Exp. 2, where all mice were equally given the diet containing 45 ppm iron from ferrous sulfate for 21 days. Mice were fed the diet and deionized distilled water at arbitrary, and were kept in an environment of 22°C and a 12-hour light/dark cycle. The average daily feed intake during gestation was recorded. The number of litters and the sex ratio were recorded and calculated. At the

finish of the experiment, the offspring mice were sacrificed after fasting for 12 h, and samples were obtained for further analysis.

2.5. Enzyme-linked immunosorbent assay (ELISA)

The contents of 5-HT (serotonin), γ-aminobutyric acid (GABA), brain-derived neurotrophic factor (BDNF), dopamine (DA), myelin basic protein (MBP) and synaptophysin (SY) in mice brain tissues were measured by the commercial ELISA kits (eBioscience, San Diego, CA, USA) according to the manufacturer's guidance.

2.6. Measurement of the iron concentration

Atomic absorption spectroscopy (AAS, HITACHI Z-2000, Japan) was used to assess the iron concentration in serum at 248 nm. Briefly, the standard solution was prepared by diluting a 1 g/L iron solution with 1% HNO_3 solution. Samples were prepared by adding 1% HNO_3 solution (300 mL) to iron solution (300 mL). Then the 40 uL sample was injected into the apparatus.

2.7. Morris water maze test

The Morris water maze test was performed on offspring mice at days 57-62 of the Exp. 2, in order to assess their spatial learning and memory ability. And the procedures were followed a previous study with minor modifications[18]. The water maze pool (120 cm in diameter and 60 cm in height) was designed into four equal-sized quadrants with a water depth of 30 cm. A platform was placed in quadrant IV, submerged 1 cm below the water surface. Water was whitened with powdered milk to keep it opaque. During the positioning navigation test, mice were placed in water in all four quadrants in a fixed order and allowed to swim for as much as 100 seconds to escape to the hidden platform. The time it took mice to climb up the platform was recorded for each trail, which was the escape latency. Four trials were conducted on each test day for five consecutive days. On day 62 of the Exp. 2, a spatial exploration test was conducted by removing the platform. The distance and time it took mice to cross the quadrant and the times of mice crossed the quadrant where the platform had previously been within 100 seconds was recorded.

2.8. Hematoxylin and Eosin (H&E) staining

The brain tissues were separated and then fixed in a 4% paraformaldehyde solution. Tissues were then paraffin-embedded and cut into thick slices in 5 μm. The sections were subjected to dewaxing three times in xylene for 5 minutes each, and then exposed to anhydrous ethanol for 5 minutes, followed by sequentially immersed in 90% ethanol, 70% ethanol, and distilled water for 5 minutes each time. Afterward, the sections were stained with H&E staining, and microscope images were captured to assess the hippocampal morphology.

2.9. Immunofluorescence staining

The brain sections (5 μm thick) were fixed, permeabilized, and blocked with 5% goat serum (Solarbio, Beijing) for 30 min. Then sections were incubated with primary antibody at 4℃ overnight. Following a thorough wash, sections were incubated with secondary antibody at room temperature for 1 h. Finally, cell

nuclei were counterstained with 4'6-diamidino-2-phenylindole (DAPI, Biosharp, Beijing, China). The hippocampal regions were visualized with confocal laser-scanning microscopy (FLUOVIEW FV1000, Olympus, Japan). Primary antibodies including GAFP, Iba-1 and NeuN were purchased from Abcam (Cambridge, UK).

2.10. 16S rRNA gene sequencing

16S rRNA gene sequencing procedure followed our earlier investigation[28]. The microbial DNA was extracted from mice feces and colonic contents by the DNA Stool Mini Kit (Qiagen, Hilden, Germany). The 16S rRNA genes in the V3-V4 region were amplified using primers 341F (5′-CCTAYGGGRBGCASCAG-3′) and 806R (5′-GGACTACHVGGGTWTCTAAT-3′) with the barcode. The amplification products were purified, quantified, and mixed in equidensity ratios for sequencing on an Illumina NovaSeq platform by Wekemo Tech Co., Ltd (Shenzhen, China). Raw data was stored in NCBI SRA database with the accession number PRJNA1150561.

2.11. Short-chain fatty acids (SCFAs) detection

Feces and colonic contents (0.2 g) were obtained and homogenized in double-distilled water (2 mL). Next, the upper solution was collected after centrifugation at 15,000 rpm for 10 minutes, then filtered through a 0.22 μm microporous membrane. SCFAs were analyzed using the gas chromatography (Agilent 7890B-5977A, USA). Generally, 1 μL of the fecal sample solution was accurately aspirated for injection, and the injector temperature was set at 230℃. Helium was employed as the carrier gas with a split ratio of 30:1, and a flow rate of 1.0 mL min^{-1} was sustained.

2.12. Metagenome sequencing

Genomic DNA was extracted and sequenced on an Illumina NovaSeq 6000 platform. Raw data was preprocessed using Kneaddata software. To acquire the high-quality clean reads, the sequencing adapters, the reads with the low quality bases (lower than 20), and the sequences with final length less than 50 bp were removed based on Trimmomatic. Human reads were further filtered to exclude the host pollution. The species contained in all samples were classified by kraken2 and then Bracken was utilized to assess the relative abundance of species at different phylogenetic levels. The gene abundance table was acquired based on the correspondence between the Uniref90 ID and the Kyoto Encyclopedia of Genes and Genomes (KEGG) database. Raw data was stored in NCBI SRA database with the accession number PRJNA1150979.

2.13. RNA-seq

Total RNA was extracted from mice brain tissues using an RNA extraction kit (Takara, UKY, Japan). After cDNA synthesis and purification, the cDNA was amplified to obtain the final library and sequenced. Raw data was processed by Wekemo Tech Co., Ltd. (Shenzhen, China) to remove the low-quality reads. Reads from the obtained samples were normalized by DESeq, and KEGG pathway enrichment analysis was conducted with a significance threshold of $P < 0.05$. Raw data was stored in NCBI SRA database with the accession number PRJNA1369803.

2.14. Cell cluture and treatment

HT-22 cells were maintained in the following medium: DMEM (Hyclone, South Logan, UT, USA) supplemented with 10% fetal bovine serum, 100 μg/mL of streptomycin and 100 U/mL of penicillin, cultured in a constant temperature incubator (Thermo Fisher Scientific, Waltham, MA, USA) at 37℃ in a humidified environment with 5% CO_2. HT-22 cells were seeded in 6-well culture plate and cultured overnight (1 x 10^6 cells/well). 20 mM sodium butyrate was then applied to HT-22 cells for 24 hours. After 24 hours, the cells were lysed using 1% sodium dodecyl sulfate (SDS) lysis buffer and conducted the subsequent analysis.

2.15. Western blot

Proteins were extracted from the mice brain and HT-22 cells, and quantified by bicinchoninic acid (BCA). After gel electrophoresis, transmembrane, blocking, incubation of primary and secondary antibodies, blots were incubated in efficient chemiluminescence (ECL) reagents and scanned by Gel Image system, and were finally quantified by ImageJ software (NIH, Bethesda, MD, USA). Primary antibodies including transferrin receptor protein 1 (TFRC), enolase 3 (ENO3), glucose transporter 1 (GLUT1) and glyceraldehyde-3-phosphate dehydrogenase (GAPDH) were purchased from Abcam (Cambridge, UK).

2.16. Real-time quantitative polymerase chain reaction (RT-qPCR)

RT-qPCR analysis based on a previous study with slight modifications[29]. cDNA was synthesized utilizing 1 μg total RNA and the PrimeScript RT reagent Kit With gDNAEraser for qPCR reverse transcription (Takara, UKY, Japan). The qRT-PCR analyses were performed on an applied biosystems 7500 fast real-time PCR system (ABI) utilizing the ArtiCanATM SYBR qPCR Mix (Tsingke, Beijing, China). An internal control (*Gapdh* gene) was utilized to normalize the variance of samples. All primer sequences of the target genes were listed in Supplementary Table S1.

2.17. Statistical Analysis

Except for the average latency in the Morris water maze test was analyzed by Two-way ANOVA, other multiple comparisons of continuous variables were performed by One-way ANOVA with Tukey test. Kruskal-Wallis H test was applied to assess the variations in microbiota. And GraphPad Prism 8.0 software was used for graphical presentation. A p value of $P < 0.05$ was regarded statistically significant and $0.05 \leq p \leq 0.10$ indicated a trend of difference. All data are presented as means ± standard error of mean (SEM).

3. Results

3.1 Structural characterization of N,O-CMCS and the N,O-CMCS-iron complex

The ^{1}H-NMR spectrum chemical shift signal of N,O-CMCS was shown in Fig. 1A. δ = 3.79 ppm corresponded to the absorption peak of the H-linked-C1, and δ = 2.26 ppm represented the absorption peak of the H-linked-C2, which is attached to the amino group. δ = 3.35 ppm was the absorption peak of the H-linked-C6. The H-linked-C3, H-linked-C4, and H-linked-C5 overlapped between δ = 3.16 - 2.85 ppm. It was found that carboxymethylation substitution of the sample mainly occurred on the amino group (C2) and

the hydroxyl group (C3 and C6), where the hydroxyl substitution was at δ = 3.66 ppm, and the amino substitution was at δ = 3.32 ppm. By integrating the area of hydroxyl- and amino-substituted carboxymethyl methylene groups respectively, the DS of the sample was calculated as 0.86 which is in part 0.44 O-site and 0.42 N-site. In addition, a small amount of residual acetyl-terminal methyl chemical shift signal was observed at δ = 1.14 ppm, and the DD of N,O-CMCS was determined to be 98%. Based on data from potentiometric titration, the estimated percentage of the deacetylation of N,O-CMCS was around 88.23%, and the estimated percentage of the carboxymethyl substitution was around 84.47%, which could be a validation of the ^{1}H-NMR analysis.

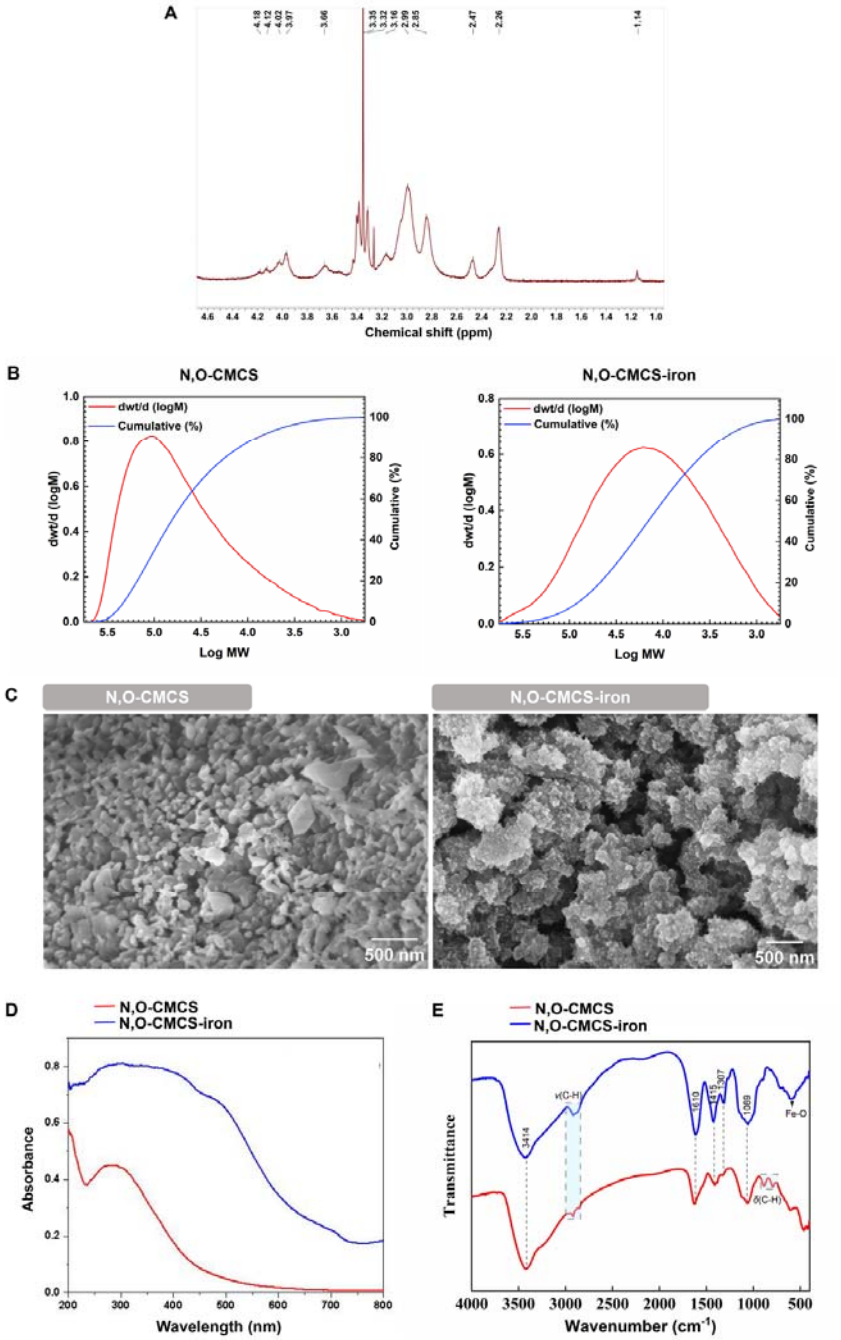


Fig. 1. Characterization of N,O-carboxymethyl chitosan (N,O-CMCS) and N,O-CMCS-iron. A) The hydrogen nucleus magnetic resonance spectroscopy (^{1}H NMR) of N,O-CMCS. B) The molecular weight. C) The scanning electron microscope (SEM) images. The scale bar is 500 nm. D) The absorbance of N,O-CMCS and N,O-CMCS-iron in ultraviolet range. E) The Fourier transform infrared (FT-IR) spectrum.

As depicted in Fig. 1B, the HPGFC analysis revealed the Mw of 87.57 kDa and the Mn of 17.95 kDa for N,O-CMCS, and the Mw of 33.51 kDa and the Mn of 6.14 kDa for N,O-CMCS-iron. From Fig. 1C, it can be seen that the surface of N,O-CMCS was uniformly smooth and more compact, while the surface of N,O-CMCS-iron was rough. In addition, N,O-CMCS-iron exhibited aggregation into clusters and became less dense. By the full-wavelength UV scans in the wavelength range of 200-800 nm, we found that the absorbance of N,O-CMCS-iron in the UV region was significantly higher than that of N,O-CMCS (Fig. 1D). FT-IR was also used to analyze the chemical structure of N,O-CMCS and N,O-CMCS-iron (Fig. 1E). The characteristic peaks at 3414, 2900 and 1610 cm^{-1} were the O-H stretching vibration, the C-H stretching vibration, and the C=O stretching vibration, respectively. In addition, the peak at 1415 cm^{-1} was the C-H bending vibration, and the peaks at 1307 and 1069 cm^{-1} were the C-O stretching vibrations. By comparing the infrared spectra of N,O-CMCS and N,O-CMCS-iron, it can be found that the strength of each characteristic peak of N,O-CMCS-iron was increased, and a wider characteristic peak appeared in the low-frequency metal-oxygen bond region, which may be related to the vibration of Fe-O. The appearance of this characteristic peak indicated that Fe^{2+} may form a coordination bond with C-O. In addition, there are also lone pairs of electrons in C=O at 1610 cm^{-1}, which can also form coordination bonds with Fe^{2+}. Therefore, it is inferred that Fe^{2+} and N,O-CMCS are bound by coordination bonds.

3.2 Effect of maternal N,O-CMCS-iron intake on serum iron concentration in dams and their offspring in Exp. 1

The overall experimental design was briefly shown in Fig. 2A. There was no obvious change in feed intake during gestation among the three groups ($p \geq 0.05$). In addition, the results suggested that the amount of fetuses, and the females to males ratio of fetuses were not statistically different among the three groups ($p \geq 0.05$) (Supplementary Table S2). In order to confirm the iron supplementation effect of N,O-CMCS-iron, the serum iron level was measured in dams and their offspring at weaning. As shown in Fig. 2B, compared with the LI group, the addition of ferrous sulfate and N,O-CMCS-iron both significantly increased the serum iron concentration of dams ($P < 0.001$). And importantly, the CI group had greater serum iron level than the NI group ($P = 0.030$), suggesting that N,O-CMCS-iron had a higher iron supplementary efficiency. A similar trend was observed in the offspring, where the serum iron levels of the offspring mice in the NI and CI groups were significantly elevated compared to the LI group ($P < 0.001$), with the CI group showing a further advantage over the NI group ($P = 0.015$).

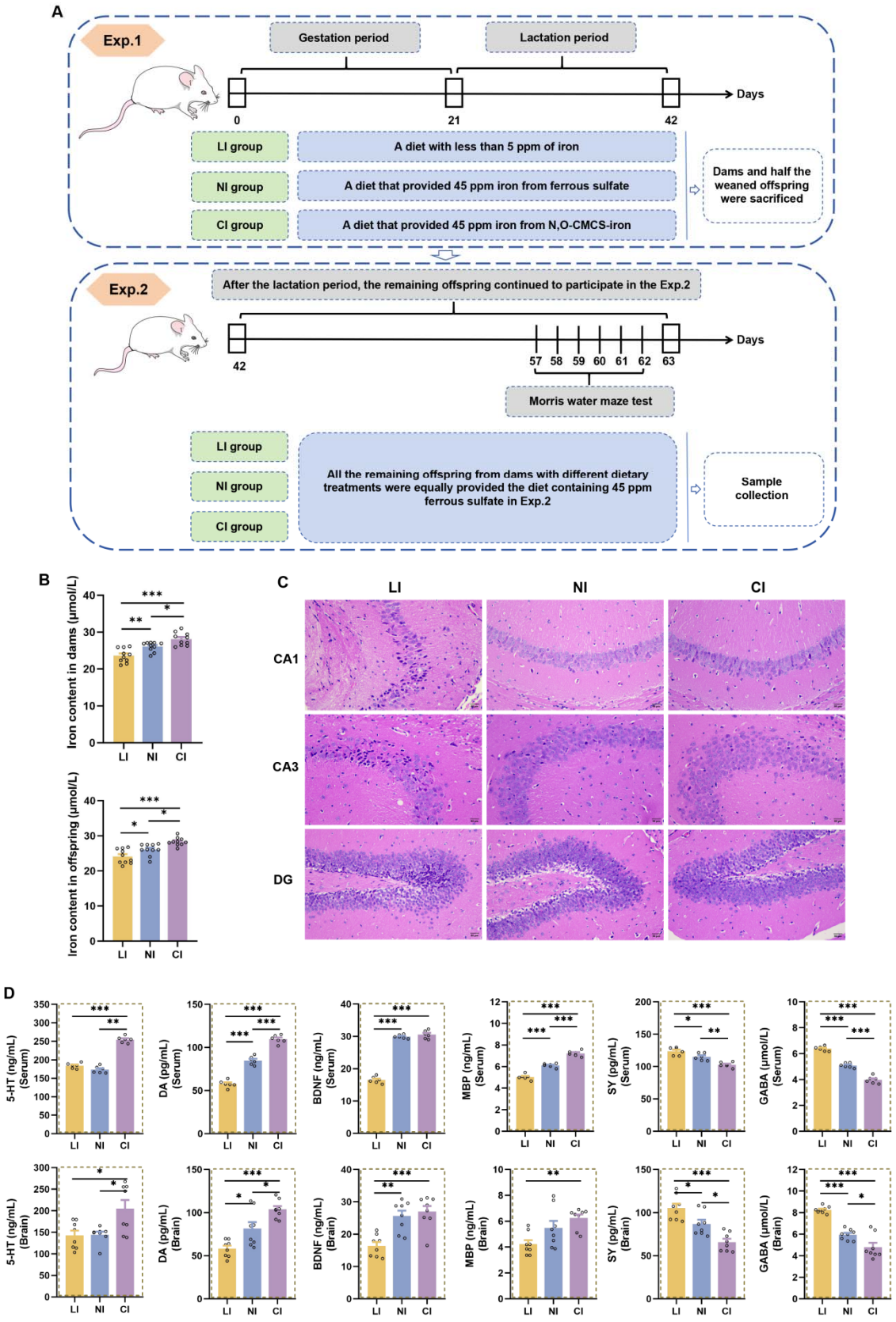


Fig. 2. Effects of N,O-carboxymethyl chitosan (N,O-CMCS)-iron on the iron concentration and cognitive function in mice in Exp. 1. A) The schematic diagram of animal experimental procedure. B) The serum iron content in dams and their offspring. (n = 10). C) The hippocampal tissue morphology of the offspring mice. The scale bar is 50 μm. (n = 10). D) The levels of neuroplasticity-related molecules in serum and brain of the offspring mice (n = 6 and 8, respectively). 5-HT: serotonin; DA: dopamine; BDNF: brain-derived neurotrophic factor; MBP: myelin basic protein; SY: synaptophysin; GABA: γ-aminobutyric acid. LI, the group in which dams ingested a low dose of ferrous sulfate. NI, the group in which dams ingested a normal dose of ferrous sulfate. CI, the group in which dams ingested N,O-CMCS-iron. * $P < 0.05$, ** $P < 0.01$, *** $P < 0.001$.

3.3 Effect of maternal N,O-CMCS-iron intake on brain cognitive function of the weaned offspring mice in Exp. 1

We next investigated the histological changes of mice hippocampus tissues by H&E staining. When mothers consume the iron-deficient diet during pregnancy and lactation, the cells in the hippocampal area of the offspring mice were loose and disorganized, with some nuclei shrinking and some neurons lost. However, the hippocampal structure of the offspring mice from mothers that ingested ferrous sulfate or N,O-CMCS-iron were obviously tight and intact (Fig. 2C). Fig. 2D illustrated the expression of neurotransmitters and proteins related to nervous system function in the offspring mice. Compared with the LI group, the offspring mice from the NI and CI groups had higher serum levels of DA ($P < 0.001$), BDNF ($P < 0.001$) and MBP ($P < 0.001$), and lower serum levels of SY ($P < 0.001$) and GABA ($P < 0.001$). And the levels of serotonin (5-HT) ($P < 0.001$), DA ($P < 0.001$) and MBP ($P < 0.001$) were higher while the levels of SY ($P = 0.003$) and GABA ($P < 0.001$) were lower in serum of the CI group than those of the NI group. Consistent with the serum alterations, the offspring mice from the LI group exhibited a significant rise in brain SY ($P < 0.001$) and GABA levels ($P < 0.001$), however there was a significant drop in brain levels of DA ($P < 0.001$), BDNF ($P < 0.001$) and MBP ($P = 0.006$). And relative to the NI group, the offspring mice from the CI group displayed the decreased amounts of SY ($P = 0.011$) and GABA ($P = 0.012$), but the increased levels of 5-HT ($P = 0.014$) and DA ($P = 0.018$) in brain.

3.4 Effect of N,O-CMCS-iron intake on fecal flora of the pregnant dams in Exp. 1

Given the critical role of gut homeostasis in brain function[30], we compared the differences in gut microbiome composition among groups of dams, as well as groups of the offspring at different stages. 16S rRNA gene sequencing revealed that N,O-CMCS-iron consumption significantly altered the maternal gut microbiota composition. In Fig. S1A, the PCoA plot analysis at the genus level exhibited that the microbial communities of the CI group was distinct from those of the other two groups. At the phylum level, Firmicutes, Bacteroidetes and Proteobacteria dominated the gut microbiota of each group. The CI group showed a significant increase in Bacteroidetes when compared to the LI and NI groups ($P = 0.001$). And the CI group showed a decrease in Firmicutes when compared to the LI group ($P = 0.004$) (Fig. S1B and E). At the family level, we found that the CI group had a higher content of the lower taxa of the phylum Bacteroidetes than the LI and NI groups did, which included family S24-7 ($P = 0.035$) and Bacteroidaceae ($P = 0.002$) (Fig. S1C and E). At the genus level, the pregnant mice in the CI group had higher abundance of *Bacteroides* ($P = 0.002$) and *Butyricimonas* ($P = 0.006$) than the LI and NI groups, and had the enhanced enrichment of *Erysipelotrichaceae_Clostridium* ($P = 0.033$) and *Blautia* ($P = 0.046$) when compared with the LI group (Fig. S1D and E). We did not find appreciable variations in gut microbiome composition between the LI and NI groups at all levels ($p \geq 0.05$). These results strongly suggested that consumption of N,O-CMCS-iron during pregnancy significantly regulated the gut microbiota structure of dams.

3.5 Effect of N,O-CMCS-iron intake on intestinal flora of the lactating dams in Exp. 1

We also looked into the impact of continued N,O-CMCS-iron supplementation on the gut flora of nursing mothers. Fig. 3A illustrated that the microbial community at the genus level in the CI group remained distinct from the other two groups. At the phylum level, the CI group had a higher relative abundance of Bacteroidetes compared to the LI and NI groups (P = 0.011) (Fig. 3B and E). At the family level, compared to the lactating mice in the LI and NI groups, Bacteroidaceae was significantly enriched in mice consumed N,O-CMCS-iron (P < 0.001) (Fig. 3C and E). And at the genus level, *Bacteroides* (P < 0.001), *Butyricimonas* (P = 0.008) and *Clostridium* (P = 0.016) were more abundant in the CI group in comparison to the LI and NI groups (Fig. 3D and E). In addition, the abundance of *Erysipelotrichaceae_Clostridium* was higher in the CI group than that in the NI group (P = 0.031) (Fig. 3D and E). Interestingly, we noticed that the differences in gut microbiota composition between the LI and the NI groups remained very small ($p \geq 0.05$).

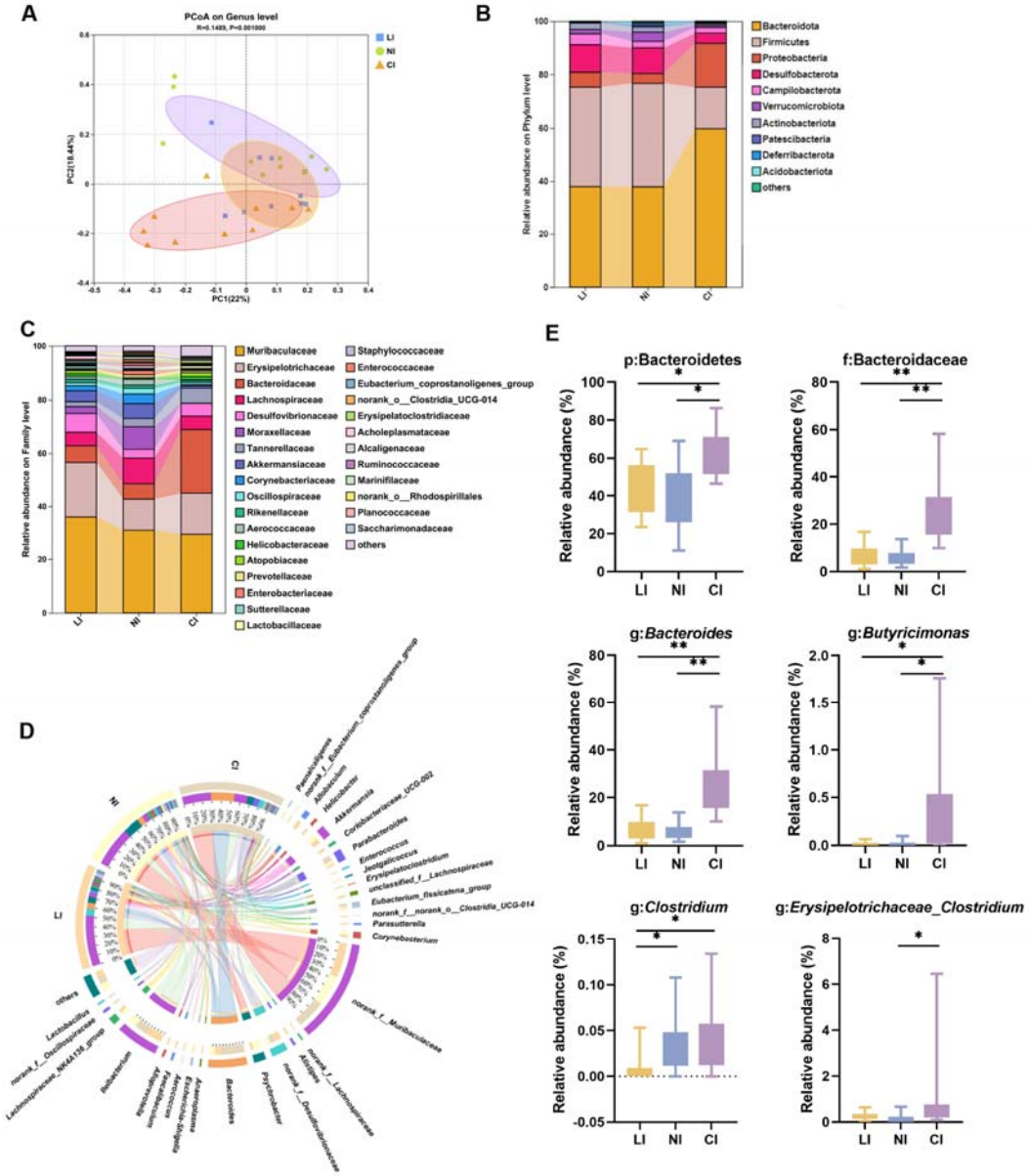


Fig. 3. Effect of N,O-carboxymethyl chitosan (N,O-CMCS)-iron on intestinal flora of the lactating mice in Exp. 1. A) The PCoA plot analysis. B-C) The barplot analysis of the fecal microbiota on the phylum and family levels. D) The chord diagram of the colonic microbiota on the genus level. E) The significant difference of microbiota across levels. LI, the group in which dams ingested a low dose of ferrous sulfate. NI, the group in which dams ingested a normal dose of ferrous sulfate. CI, the group in which dams ingested N,O-CMCS-iron. (n = 10). * P < 0.05, ** P < 0.01, *** P < 0.001.

3.6 Effect of maternal N,O-CMCS-iron intake on intestinal flora of the weaned offspring mice in Exp. 1

In view of the influence of maternal microbes on their offspring, we analyzed the intestinal microbiota structure of the weaned offspring mice. Interestingly, the trend of differences in gut microbiome composition among the offspring mice of each group was consistent with that of their mothers. The offspring in the CI group exhibited a microbial community structure that was distinct from and more favorable than that of the LI and NI groups (Fig. 4A). And specifically, within the phylum level, the weaned offspring mice from dams ingesting N,O-CMCS-iron showed a significant increase in Bacteroidetes (P = 0.015) and a decrease in Firmicutes (P = 0.001) compared to those from dams in the other two groups (Fig. 4B and E). Within the family level, in comparison with the LI and NI groups, the offspring mice from the CI group had the higher abundance of Bacteroidaceae (P < 0.001) (Fig. 4C and E). In addition, the offspring mice from the CI group had the higher abundance of Clostridiaceae than those from the LI group (P = 0.010) (Fig. 4C and E). And within the genus level, the relative abundances of *Bacteroides* (P < 0.001), *Erysipelotrichaceae_Clostridium* (P = 0.006), *Clostridium* (P = 0.001) and *Butyricimonas* (P = 0.001) were markedly elevated in the offspring mice whose mothers have received N,O-CMCS-iron (Fig. 4D and E). Our results further supported the vertical transmission effect of gut microorganisms between mothers and their offspring.

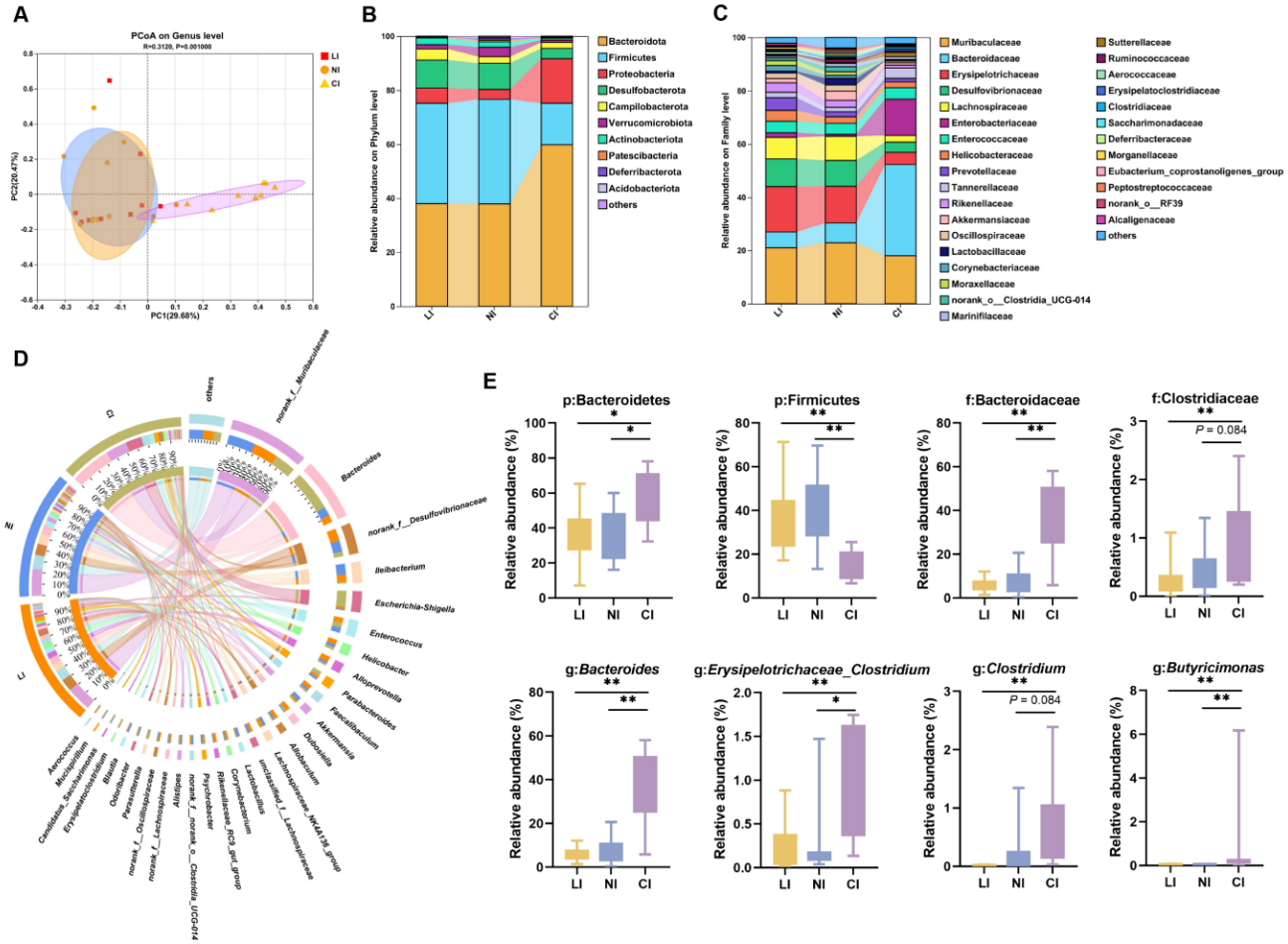


Fig. 4. Effect of N,O-carboxymethyl chitosan (N,O-CMCS)-iron on intestinal flora of the weaned offspring mice in Exp. 1. A) The PCoA plot analysis. B-C) The barplot analysis of the colonic microbiota on the phylum and family levels. D) The chord diagram of the colonic microbiota on the genus level. E) The significant difference of microbiota across levels. LI, the group in which dams ingested a low dose of ferrous sulfate. NI, the group in which dams ingested a normal dose of ferrous sulfate. CI, the group in which dams ingested N,O-CMCS-iron. (n = 10). * P < 0.05, ** P < 0.01, *** P < 0.001.

3.7 Effect of maternal N,O-CMCS-iron intake on SCFAs contents of dams and their offspring in Exp. 1

Fig. 5 displayed the amounts of SCFAs in feces or colonic contents of dams and their offspring. Consistent with the observed microbiota shifts, we found that at the end of gestation, the fecal butyrate concentration of dams in the N,O-CMCS-iron intake group was markedly higher than that in the LI and NI groups (P = 0.001) (Fig. 5A). The concentrations of acetate, propionate, isobutyrate, valerate and isovalerate had no significant changes among all groups ($p \geq 0.05$) (Fig. 5A). And at the end of the lactation period, dams in the CI group also showed the increased butyrate level of the colonic content when compared with the other two groups ($P < 0.001$) (Fig. 5B). Moreover, we revealed that the offspring mice from the CI group had a greater butyrate level than the LI and NI groups ($P < 0.001$) (Fig. 5C).

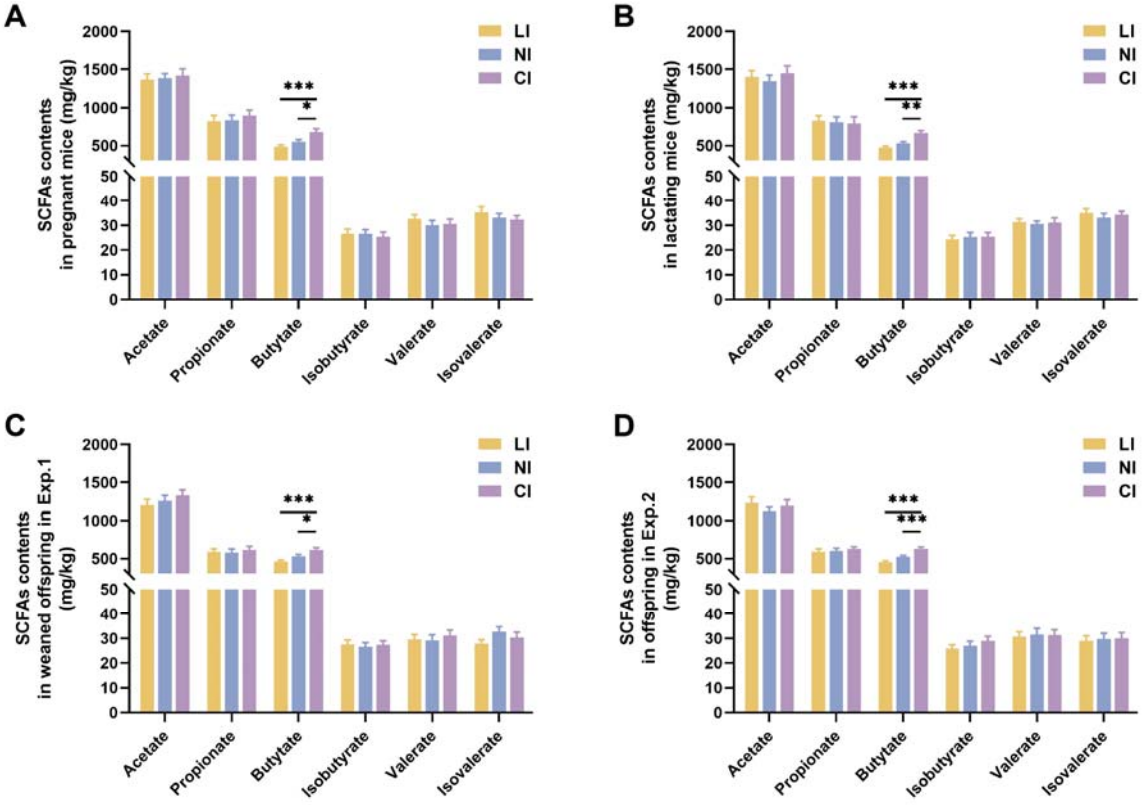
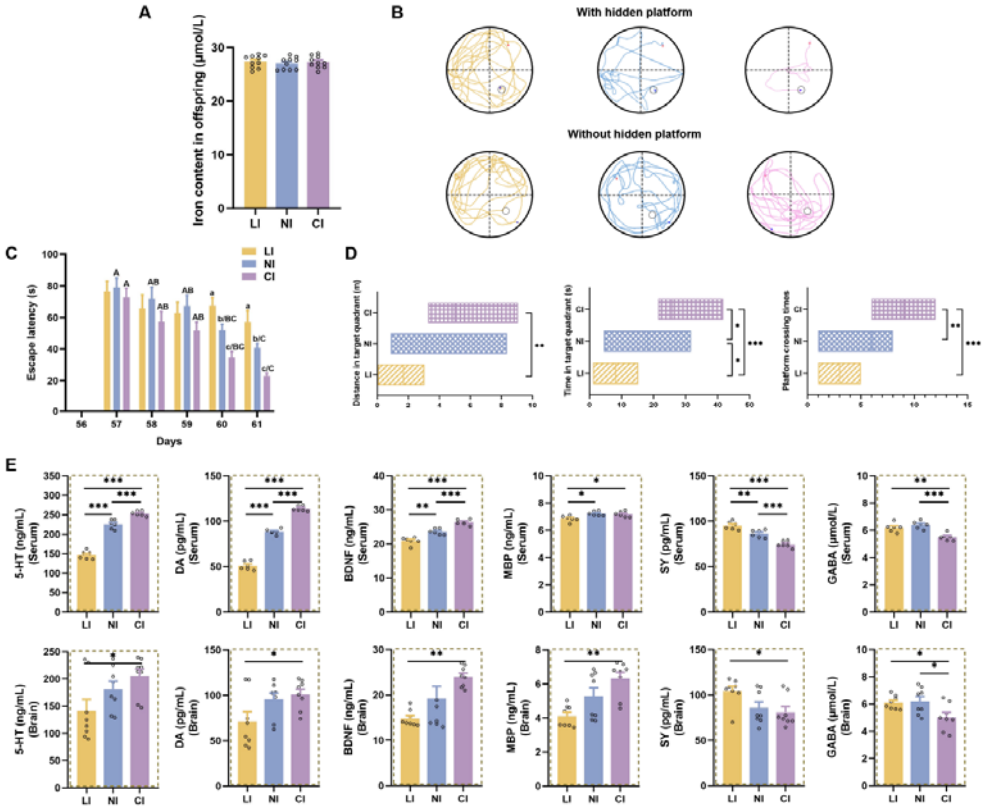


Fig. 5. N,O-carboxymethyl chitosan (N,O-CMCS)-iron enhanced the colonic butyrate content in dams and their offspring. A) The concentrations of short-chain fatty acids (SCFAs) in the colon of the pregnant dams in Exp. 1. B-C) The concentrations of SCFAs in the colon of the lactating dams and the weaned offspring mice in Exp. 1. D) The colonic SCFAs concentrations in the offspring mice in Exp. 2. LI, the group in which dams ingested a low dose of ferrous sulfate. NI, the group in which dams ingested a normal dose of ferrous sulfate. CI, the group in which dams ingested N,O-CMCS-iron. In Exp. 2, the offspring mice from the three groups all received ferrous sulfate equally. (n = 10). * $P < 0.05$, ** $P < 0.01$, *** $P < 0.001$.

3.8 The serum iron level and brain cognitive function of the weaned offspring mice treated with ferrous sulfate for 3 weeks in Exp. 2

In Exp. 2, all offspring were switched to a standard ferrous sulfate diet for 3 weeks. As depicted in Fig. 6A, there was no significant difference in serum iron level across the groups ($p \geq 0.05$). The Morris water maze test was conducted to evaluate the spatial learning and memory ability of the offspring mice. The swimming trajectories in different group mice during the test phase were shown in Fig. 6B. 2-way ANOVA was used to detect the escape latency of mice. During the former 3 days of the training phase, there were no

statistically significant differences in the escape latency among three groups ($p \geq 0.05$). However, the escape latency of the NI and CI offspring mice was shorter than that of the LI offspring mice at the latter two days ($P < 0.001$) (Fig. 6B and C). And it is worth noting that the CI mice had shorter escape latency than the NI mice at the latter two days ($P = 0.030$ and 0.037, respectively), indicating a stronger learning ability of the offspring from dams treated with N,O-CMCS-iron. The escape platform was taken down after five days of training in order to assess the memory performance of the offspring mice. We saw that the LI mice spent a much less amount of time ($P = 0.003$) and distance ($P < 0.001$) in the initial platform region, as well as less crossings over the original platform position ($P < 0.001$). Moreover, relative to the offspring mice from the NI group, mice from the CI group displayed longer stay ($P = 0.027$) and more crossings ($P = 0.002$) over the target zone (Fig. 6B and D). These behavioral advantages were supported by neurochemical and histological evidence. Maternal exposure to N,O-CMCS-iron significantly modulated the levels of neurotransmitters (5-HT and GABA) and proteins related to nervous system function (DA, BDNF, MBP and SY) in serum and brain of the offspring mice ($P < 0.05$) (Fig. 6E). We also performed immunostaining analysis for GFAP (a marker for reactive astrocytes), Iba-1 (a marker for macrophage and microglial activation), and NeuN (a marker for neurons) in the hippocampus of mice brain. As demonstrated in Fig. 6F, compared with the LI group, the offspring mice from the NI and CI groups had higher $NeuN^+$ cells ($P < 0.001$), and lower $GFAP^+$ ($P < 0.001$) and $Iba\text{-}1^+$ cells ($P < 0.001$) in the hippocampus. Furthermore, the offspring mice from the CI group showed the increased $NeuN^+$ cells ($P < 0.001$) and the declined $GFAP^+$ cells ($P = 0.012$) than those from the NI group. These results interestingly suggested that consumption of N,O-CMCS-iron by mothers during pregnancy and lactation enhanced the cognitive function of their offspring, which was superior to that of the offspring from the other two groups, even if all offspring had received the same diet for a period of time.



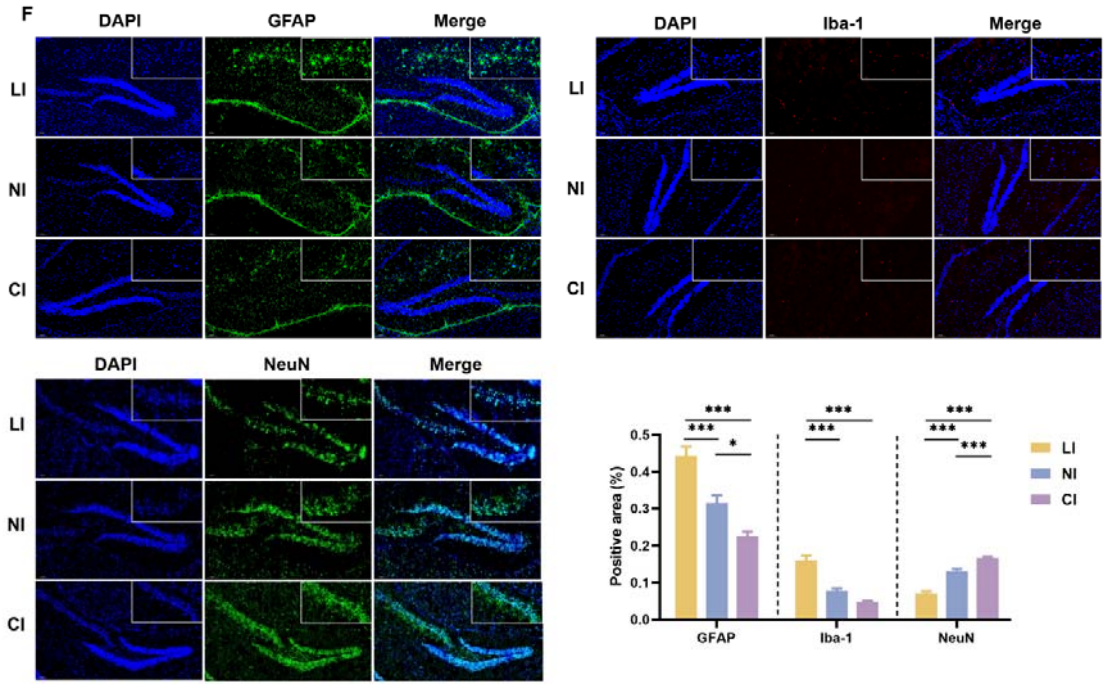


Fig. 6. The iron level and brain cognitive function of the offspring mice in Exp. 2. A) The serum iron concentration of the offspring mice in each group after 3 weeks of equal ferrous sulfate treatment. (n = 10). B) Representative swimming trajectories of the offspring mice in the navigation test (upper) and the space exploration test (lower). The little circle marks the starting point. C) The average escape latency of the offspring mice in the navigation test. Capital letters represented the comparisons of the same treatment group over different days, and lowercase letters represented the comparisons among different treatment groups at the same time point. The same letters indicated no significant difference. D) The distance, time spent, and crossing numbers in the target quadrant of the offspring mice in the space exploration test. (n = 8). E) The contents of neuroplasticity-related molecules in serum and brain of the offspring mice. (n = 6 and 8, respectively). F) Representative immunofluorescence images and quantification of $GFAP^+$, $Iba\text{-}1^+$ and $NeuN^+$ cell populations in the DG of hippocampus. (n = 3). 5-HT: serotonin; DA: dopamine; BDNF: brain-derived neurotrophic factor; MBP: myelin basic protein; SY: synaptophysin; GABA: γ-aminobutyric acid. The offspring mice from the three groups all received ferrous sulfate equally in Exp. 2. * $P < 0.05$, ** $P < 0.01$, *** $P < 0.001$.

3.9 The intestinal flora composition of the offspring mice in Exp. 2

To further verify the importance of gut flora composition in the improvement of brain function by N,O-CMCS-iron, we then performed metagenomic sequencing on the colonic contents of the offspring mice in Exp. 2. The relative abundance at different phylogenetic levels was contrasted among the three groups. The Principal component analysis (PCA) on the genus level showed that the CI group had the distinguishable microbiota composition when compared to the other two groups (Fig. 7A). Overall, the gut microbial communities across all groups were dominated by the phylum Bacteroidetes and Firmicutes, with Verrucomicrobia and Proteobacteria following closely behind. The CI group showed a larger abundance of Bacteroidetes in comparison to the LI and NI groups (P = 0.002) (Fig. 7B and C). At the family level, a similar composition pattern was noted. The relative abundance of Bacteroidaceae was considerably higher in mice in the CI group (P = 0.002). In addition, Clostridiaceae showed an increasing trend in the CI group when compared to the LI group (P = 0.058) (Fig. 7B and C). And at the genus level, the contents of *Butyricimonas* (P = 0.029) and *Clostridium* (P = 0.024) were significantly enhanced in the CI group. Furthermore, the content of *Bacteroides* was increased in the CI group (P = 0.014) (Fig. 7B and C). The metagenomics analysis revealed significant improvements in the gut microbiome composition of the offspring mice from dams

treated with N,O-CMCS-iron during pregnancy and lactation, which provides further indication of the inheritance and colonization of the microbiota during early life, as well as the possible role of the maternal nutritional status in influencing the offspring brain development through modifying the vertical transmission of gut microbiota.

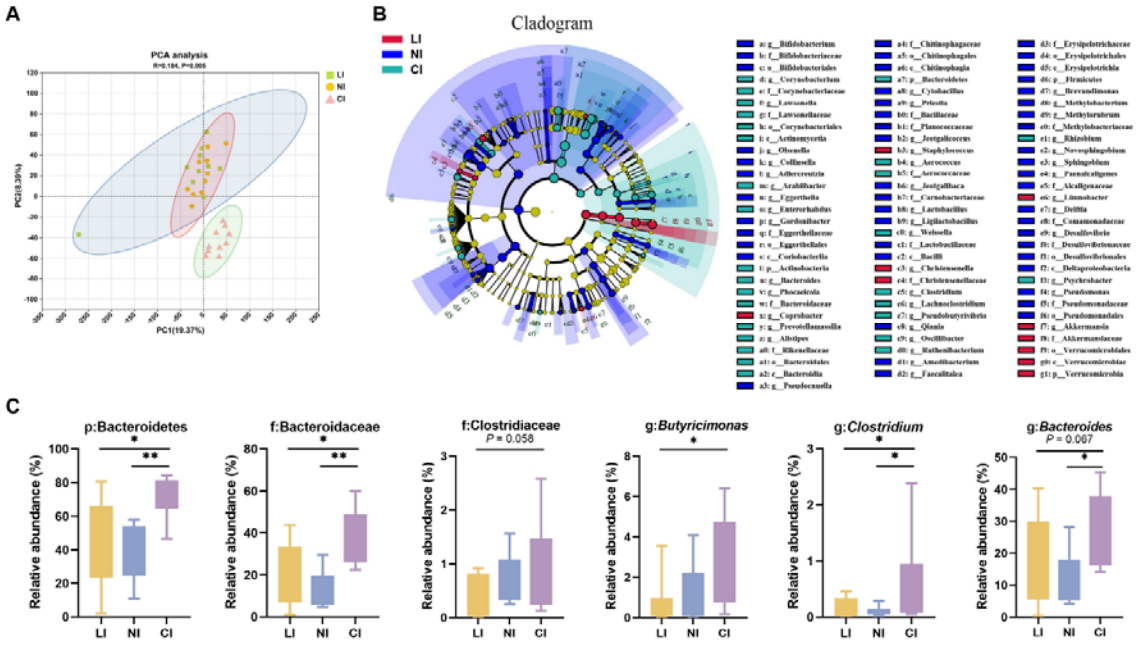


Fig. 7. The intestinal flora composition of the offspring mice in Exp. 2. A) The Principal component analysis (PCA) plot of the colonic microbiota on the genus level. B) Indicator bacteria with LDA scores of 2 or greater after FDR correction in bacterial communities of the offspring mice among the three groups. C) The significant difference of the colonic microbiota on the phylum, family and genus levels. The offspring mice from the three groups all received ferrous sulfate equally in Exp. 2. (n = 10). * $P < 0.05$, ** $P < 0.01$, *** $P < 0.001$.

3.10 The functional characteristics of microbiota of the offspring mice in Exp. 2

We next analyzed the metagenomic reads using the KEGG database to examine the functional properties of the microbiota in each group. The metabolism pathway was shown to be the most prevalent of the six major KEGG pathways. Besides, 47 level 2 pathways were identified, with amino acid metabolism and carbohydrate metabolism being the most abundant (Fig. 8A). Annotated genes that were differentially abundant to the KEGG database showed that there were notable variations among groups in a number of pathways and functions. In contrast to the other two groups, the CI group exhibited a comparatively elevated degree of carbohydrate metabolism ($P < 0.001$) and lipid metabolism ($P = 0.031$) (Fig. 8B). Notably, we found a mass of KOs with significant differences in relative abundance among these three groups, and the results were shown in detail in Supplementary Fig. S2. We identified 197 KOs enriched in the CI group, 53 KOs enriched in the NI group, and 155 KOs enriched in the LI group by LEfSe (LDA > 2, $P < 0.05$). Critically, key enzymes for butyrate synthesis, phosphate butyryltransferase (K00634, $P < 0.001$) and butyrate kinase (K00929, P = 0.002), were significantly enriched in the CI group (Fig. 8C and Fig. S2). Fig. 8D revealed the species that contribute to butyrate synthesis. The dominant species enriched in CI group associated KOs, *Bacteroides vulgatus* and *Bacteroides dorei*, which are members of the Bacteroidetes phylum mainly contributed to the metabolic changes of N,O-CMCS-iron intake. These results implied that certain bacterial species engaged in

the butyrate synthesis pathway may be the driving force behind the gut microbiome's influence on brain function.

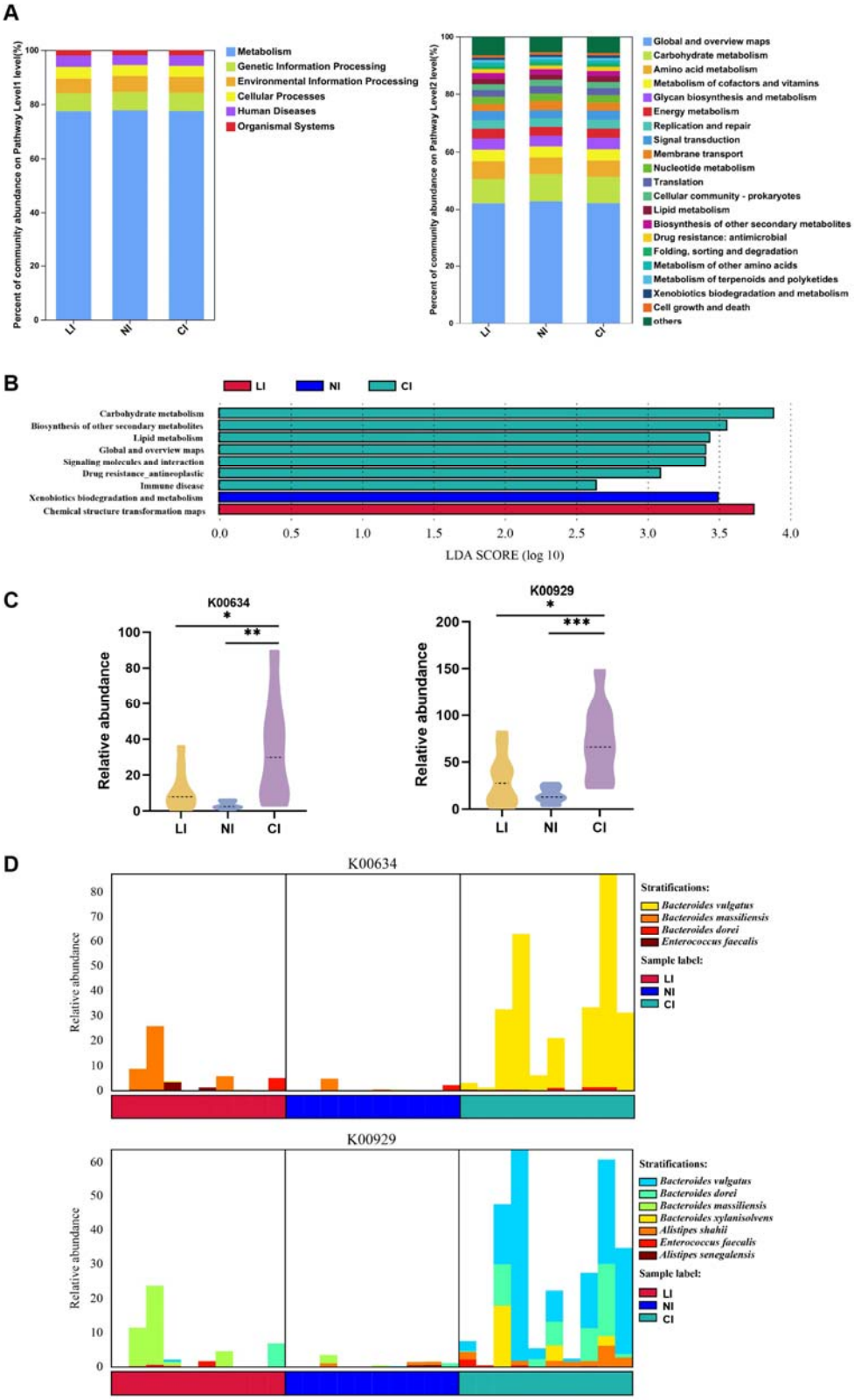


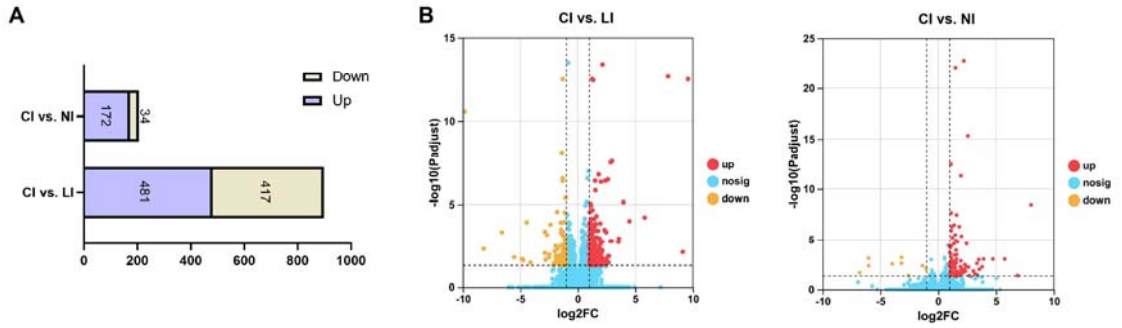
Fig. 8. The KEGG functional characteristics of microbiota of the offspring mice in Exp. 2. A) The comparative barplot of the functional KEGG among the three groups at the level 1 and level 2 pathways. B) The LEfSe analysis of the level 2 pathways of the functional KEGG among the three groups (LDA score >2.0, $P < 0.05$ after FDR correction). C) The relative abundance of phosphate butyryltransferase (K00634) and butyrate kinase (K00929) in microbial KEGG analysis. D) Species contributions to phosphate butyryltransferase (K00634) and butyrate kinase (K00929) associated with butyrate synthesis. The offspring mice from the three groups all received ferrous sulfate equally in Exp. 2. ($n = 10$). * $P < 0.05$, ** $P < 0.01$, *** $P < 0.001$.

3.11 The SCFAs contents of the offspring mice in Exp. 2

To further verify whether microbial metabolites were altered, we determined the SCFAs concentrations of the mice colonic contents by GC/MS. The colonic concentrations of acetate and propionate were not significantly different among all groups ($p \geq 0.05$) (Fig. 5D). When compared with the LI group, the level of butyrate did not differ statistically from that in the NI group ($p \geq 0.05$). Relative to the offspring mice from the LI and NI groups, however, mice from the CI group displayed an obvious elevation in butyrate ($P < 0.001$) (Fig. 5D). There were no remarkable changes in the colonic contents of isobutyrate, valerate and isovalerate among these three groups ($p \geq 0.05$) (Fig. 5D). The above results reinforced the fact that maternal N,O-CMCS-iron diet enhanced the production of butyrate in their offspring.

3.12 HIF-1α signaling was significantly altered in the offspring brain in Exp. 2

We then explored the differential mRNA in the offspring brains through RNA-seq in order to inquire the possible mechanism of maternal intake of N,O-CMCS-iron to improve the cognitive function of offspring. Fig. 9A and B uncovered the DEGs between the LI and CI groups, as well as between the NI and CI groups. It was shown that there were 898 differentially expressed genes (DEGs), of which 481 were up-regulated, and 417 were down-regulated in the CI group relative to the LI group. In addition, there were 172 genes were up-regulated and 34 genes were down-regulated in the CI group compared with the NI group. Genes that showed a fold change more than 1.2 and an FDR below 0.05 were then subjected to further KEGG analysis. We found that the HIF-1α signaling was significantly enriched in the CI group relative to both the LI ($P = 0.001$) and NI groups ($P < 0.001$) (Fig. 9C). HIF-1α is an important transcription factor, and the downstream genes it regulates play a significant role in improving cognitive function[31], thus the HIF-1α signaling may be a pivotal factor by which maternal N,O-CMCS-iron exposure affects the brain cognitive ability of their offspring. Moreover, we found that DEGs involved in HIF-1α signaling among the three groups mainly included *Edn1*, *Slc2a1*, *Tfrc*, *Angpt2*, *Ins2*, *Flt1*, *Eno3*, *Aldob* and *Vegfa* (Fig. 9D). The RT-qPCR results confirmed the findings of RNA-seq, indicating that the mRNA expression of these genes was indeed considerably increased in the CI group ($P < 0.05$) (Fig. S3A). Moreover, we randomly selected several proteins encoded by DEGs for western blot verification. As shown in Fig. S3B, the expression of downstream signal proteins of HIF-1α such as TFRC ($P = 0.012$), ENO3 ($P = 0.001$) and GLUT1 (encoded by *Slc2a1*) ($P = 0.005$) was also significantly enhanced in the CI group. The discovery of key genes could provide targets for improving the brain microenvironment and thereby strengthening the cognitive function.



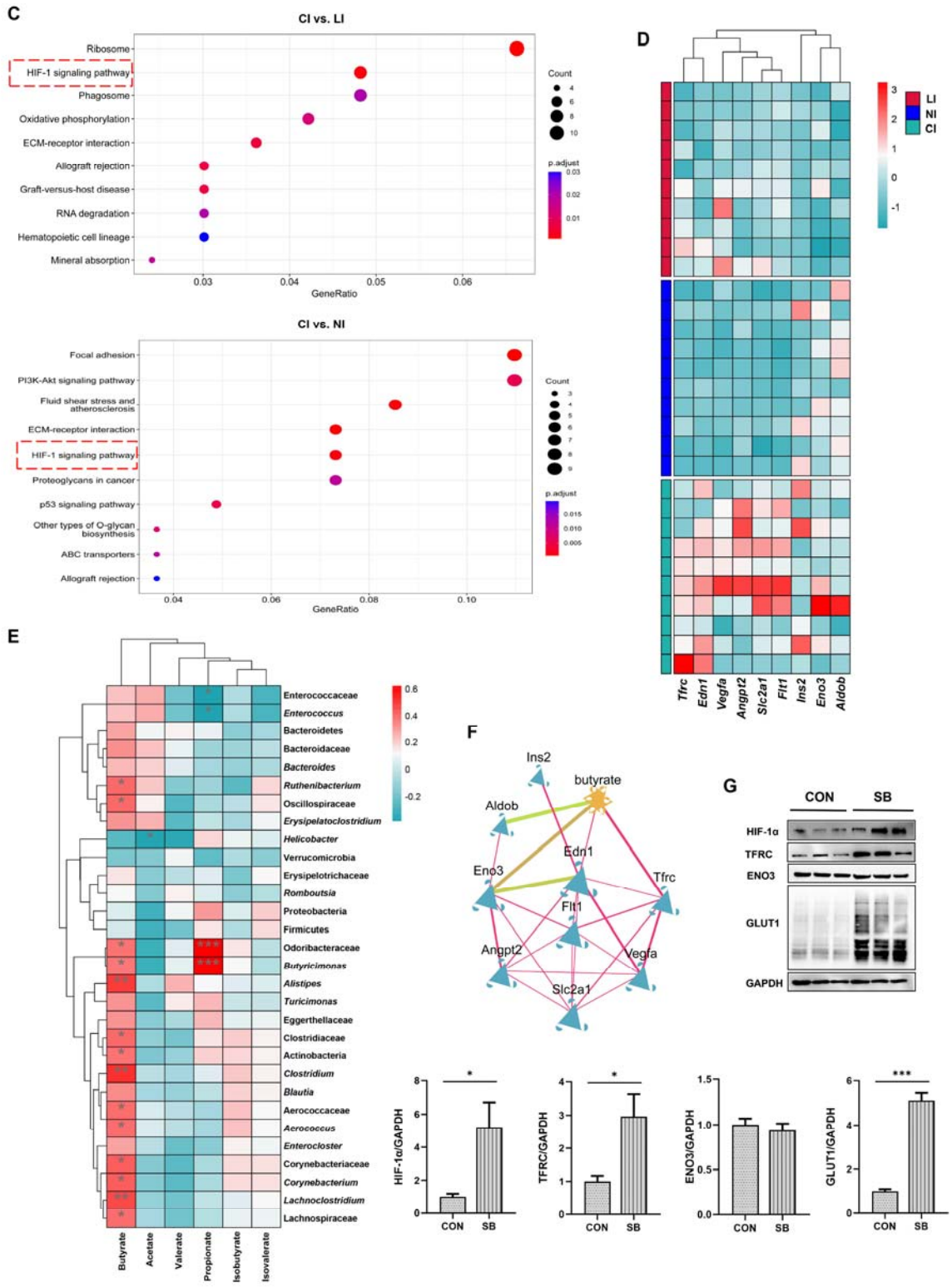


Fig. 9. The altered HIF-1α signaling was closely related to SCFAs contents in Exp. 2. A) The number of differentially expressed genes (DEGs) between the LI and CI groups, and between the NI and CI groups. B) The volcano map of DEGs between the LI and CI groups, and between the NI and CI groups. C) The KEGG and pathway enrichment analysis of the DEGs between the LI and CI groups, and between the NI and CI groups. D) The hierarchical clustering analysis of 9 DEGs involved in the HIF-1α signaling. E) The Spearman analysis of the association between the colonic bacteria and SCFAs. F) The network analysis of differential genes regulated by HIF-1α signaling and butyrate interactions. (n = 10). G) Western blot analysis of HIF-1α, TFRC, ENO3 and GLUT1 in HT-22 cells. (n = 3). CON, no treatment was carried out on the HT-22 cells. SB, HT-22 cells were treated with 20 mM sodium butyrate. LI, the the group in which dams ingested a low dose of ferrous sulfate. NI, the group in which dams ingested a normal dose of ferrous sulfate. CI, the group in which dams ingested N,O-CMCS-iron. The offspring mice from the three groups all received ferrous sulfate equally in Exp. 2. * $P < 0.05$, ** $P < 0.01$, *** $P < 0.001$.

3.13 Correlation between gut microbes and SCFAs, as well as between SCFAs and HIF-1α signaling in Exp. 2

To reveal the relationship between gut bacteria and SCFAs, and between SCFAs and HIF-1α signaling, the correlation analysis was preformed respectively. The top 30 bacteria within phylum, family and genus levels were selected for Spearman correlation analysis with SCFAs, and the results were displayed in Fig. 9E. The relative abundances of Clostridiaceae (P = 0.025), Corynebacteriaceae (P = 0.018) and Oscillospiraceae (P = 0.028) were positively related to the butyrate level. Furthermore, butyrate showed markedly positive correlations with the contents of *Clostridium* (P = 0.003) *and Butyricimonas* (P = 0.042). In addition, the abundances of Bacteroidaceae (P = 0.085) and *Blautia* (P = 0.074) showed positive associations with the butyrate level. We also analyzed the correlation between differential genes regulated by HIF-1α signaling and SCFAs. As plotted in Fig. 9F, nine DEGs were closely related to each other ($P < 0.05$). Moreover, the butyrate level had significant positive correlations with the expressions of *Tfrc* (P = 0.048) and *Edn1* (P = 0.007). Besides, the contents of *Eno3* (P = 0.082) and *Aldob* (P = 0.095) showed a trend of positive correlations with the butyrate level. In order to further verify the regulation of butyrate on HIF-1α in the brain, we conducted an in vitro experiment using the mouse hippocampal neural cell line HT-22. We found that the butyrate treatment significantly increased the protein expression levels of HIF-1α (P = 0.049) and its downstream proteins such as TFRC (P = 0.046) and GLUT1 ($P < 0.001$) in HT-22 cells. These results collectively indicated that butyrate could activate the HIF-1a signaling pathway in the brain, thereby improving the micro-environment of the brain and enhancing its cognitive function.

4. Discussion

Sufficient nutrition during pregnancy and lactation is particularly significant, as these periods are critical for fetal brain formation that lay the foundation for the development of cognition and behavior across childhood and adulthood. Poor maternal diet during pregnancy and lactation has been linked to long-term impact on the offspring, which is difficult to recover from even if the diet structure of the offspring is optimized[20]. Iron deficiency is reported to be the most frequent micronutrient deficiency worldwide, especially for pregnant women and infants with high iron demands[1]. As an imperative micronutrient, iron plays a central role in numerous neurodevelopmental processes, including hippocampus development, myelin production, and neurotransmitter synthesis, which are essential for brain function in fetuses and children[2]. Evidence from animal and in vivo studies has confirmed that iron deficiency in fetal period is strongly associated with cognitive deficits both in the short and long term[32,33], and it is claimed that host's gut microbes and their metabolites contribute to iron absorption and transport in the organs of body[12,13]. Therefore, ensuring adequate iron supply during pregnancy and lactation is crucial for optimal fetal development and infant cognition.

Polysaccharides-iron complexes have a high release rate in the gastrointestinal tract, which facilitates the body's absorption and makes them the ideal iron supplement. CMCS is one of the most important derivatives of chitosan, which has excellent solubility in aqueous media. In addition, the introduction of -COOH makes its

ability to bind metal ions greatly improved compared with chitosan[25]. Studies have shown that CMCS-based formulations have good adhesion performance and can prolong their residence time in the intestine, thus improving the bioavailability of drugs in the gastrointestinal tract[34]. N,O-CMCS is considered a highly promising biomaterial due to its favorable physical and biological characteristics, including water solubility, moisture retention, gel-formation, and biocompatibility[35]. Thus, the novel N,O-CMCS-iron complex was synthesized and the structures of the complex were revealed by FT-IR, UV scan and SEM in this study. Using a maternal iron deficiency mouse model, we further evaluated the effect of maternal N,O-CMCS-iron supplementation on cognitive function in offspring and explored the underlying mechanisms.

Iron deficiency can be categorized into two basic forms: absolute and functional iron deficiency. And absolute iron deficiency is defined as reduced or depleted plasma and body stores of iron, which is usually caused by a decrease in iron uptake or an increase in iron demand[7]. In the present study, we treated dams during pregnancy and lactation with different levels and sources of iron supplements. To assess the long-term effects of maternal iron nutrition on offspring, all offspring were switched to an identical ferrous sulfate-containing diet after weaning. As expected, we found that a low iron diet during pregnancy and lactation did decrease the serum iron concentration in mothers and their offspring in the Exp. 1, while the maternal intake of ferrous sulfate or N,O-CMCS-iron both significantly increased the serum iron concentration in themselves and pups, and N,O-CMCS-iron was more effective in iron supplementation. These results confirmed that the type of iron in maternal diet affected the iron status in the offspring. Since iron is involved in neurodevelopmental processes in the brain, the iron status in the body is inextricably linked to the brain cognitive function.

Neurotransmitters and neurotrophic factors in brain modulate cognitive performance by influencing neuroplasticity, and iron deficiency may interfere with the metabolism of these regulatory molecules. Two neurotransmitters, GABA and 5-HT, play a pivotal role in brain plasticity, which are involved in the memory and learning process of the body[36]. It is reported that iron deficiency result in increased GABA concentrations in several brain regions, including the hippocampus, globus pallidus and striatum. The elevated GABA levels indicate an increased inhibitory drive that restrains the overall neurotransmission rates and brain activity due to energy deficits[37]. Additionally, iron serves as a cofactor for tryptophan hydroxylase and tyrosine hydroxylase, enzymes critical for the synthesis of 5-HT and DA, respectively. Moderate and severe iron deficiency during pregnancy reduced 5-HT uptake by brain synaptic vesicles in offspring[38]. And the negative effect of iron deficiency on DA functions have also been reported before[32]. BDNF, one of the most broadly distributed neurotrophins in the mammalian brain, was found at a reduced level in iron-deficient rats in a previous study[39]. MBP is a major component in central nervous system myelin and is required for the adhesion of the cytosolic surfaces of multilayered tight myelin[40]. One research proved that iron deficiency produced a significant reduction in MBP[41]. In our study, the offspring mice from mothers fed with the low-iron diet, those from mothers of the NI and CI groups had higher serum and brain levels of BDNF, MBP and DA, and this continued even after all the offspring mice were given ferrous sulfate for 3 weeks after

weaning. It is worth noting that the levels of BDNF, MBP and DA in the offspring brain of the CI group were higher than those of the NI group. These findings indicated that the addition of N,O-CMCS-iron to the maternal diet during gestation and lactation promoted brain neuroplasticity of the offspring mice and outperformed inorganic iron. In addition, it is evident that poor maternal nutrition during pregnancy and lactation had a negative impact on the cognitive ability of the offspring, and even if the dietary structure of the iron-deficient offspring was optimized to restore normal iron levels, their cognitive function was hard to recover in the short term.

The hippocampus is a central hub for learning and memory. Studies in laboratory animal models have discovered that the hippocampus is extremely susceptible to iron availability, with structural and metabolic changes occurring in the hippocampal region in iron-deficient mice[2,42]. Therefore, we also assessed the histological changes of mice hippocampal tissues via immunofluorescence staining at the end of the Exp. 2. And obviously, our results showed that compared to the offspring mice from the LI and NI groups, the $GAFP^+$ and $Iba\text{-}1^+$ cells in the hippocampal region were lower while the $NeuN^+$ cells were higher in the CI group mice, indicating a suppressing efficacy of hippocampal immune cell activation and a promotion of neuronal development. Behavioral data from the Morris water maze test corroborated these histological findings. Maternal iron shortage significantly prolonged the escape latency of the offspring mice in the navigation test, and decreased the time the offspring mice spent in the target quadrant in the space exploration test. These results clearly demonstrated that maternal iron deprivation during pregnancy and lactation inhibited the cognitive function of their offspring, and that this effect had a degree of long-term potency and was not altered by short-term optimization of the diet. In alignment with our results, other studies have reported that children with chronic postnatal iron deficiency continued to have significant deficits in cognitive functions such as spatial and selective memory over a decade after treatment to restore iron stores in the body[6,33].

Comparing the two types of iron supplements, ferrous sulfate and N,O-CMCS-iron, we uncovered that the offspring of dams fed with N,O-CMCS-iron had the increased iron storage and promoted brain neuroplasticity. Even though the weaned offspring mice were all given ferrous sulfate in the Exp. 2 and the serum iron content of the offspring mice restored to the same level, the offspring mice from the CI group still performed better on behavioral test. Researches from countries around the world have yielded generally consistent results in terms of long-term outcomes, which were mainly carried out at late preschool, early school age, and adolescence. In both Chile and Costa Rica, children who suffered from chronic or severe iron deficiency during infancy had poorer performance in some certain tests of the cognitive function. For the Costa Rica sample aged between 11 and 14, it was observed that they performed poorly in tachistoscopic threshold, spatial memory, and selective attention[43]. In the follow-up study in Chile for children aged 5 and 10, as well as in a 19-year longitudinal study in Costa Rica, children with prior iron deficiency performed worse on executive function tests, especially those requiring inhibitory control and planning abilities[44,45]. Studies using animal models also have revealed that iron deficiency during gestation and lactation could lead to immediate and long-term changes in behavior and development, which helps interpret some long-term

findings in humans[46,47]. The endpoint of this study was set at the 42nd day after birth, which approximately corresponds to the late adolescence and early adulthood stage in humans. Thus, our results could indicate that N,O-CMCS-iron was more effective in supplementing iron and improving the brain cognitive function when compared with inorganic iron, and its effect was long-term to some extent.

It is interesting to explore the influence of gender differences when analyzing the relationship between iron deficiency in mothers and the cognitive function of their offspring. Three animal studies have all confirmed the brain damage in the offspring born to iron-deficient dams. Among them, the brain damage in female offspring was less severe than that in male offspring[48-50]. This might be related to the differences in placental growth during pregnancy, which plays a key role in the development of the fetal brain. Female fetuses mainly rely on the growth of the placenta, while male fetuses rely on the nutrient delivery through the placenta[51]. Therefore, when mothers experience stress or suffer from nutritional deficiencies (such as iron deficiency), the risk of delayed brain development in males is higher than females. But another study reported that the offspring of iron-deficient dams had the reduced serum iron and increased anxiety behavior in neonates, which was independent of sex[52]. To eliminate the influence of gender, in this study we used offspring that were equally divided between males and females.

A complex interplay exists between iron homeostasis and gut microbial ecology. It has been reported that low iron status could disrupt gut microbiota composition[18]. And in turn, intestinal microbial activity affects iron bioavailability and absorption[53,54]. By 16S high-throughput sequencing and metagenomics, we analyzed the microflora composition of dams and their offspring at each stage. We observed a high degree of similarity between the microbial structures of dams and their respective offspring, indicative of a vertical transmission effect. Specifically, the relative amounts of Bacteroidaceae, Clostridiaceae, as well as *Butyricimonas, Clostridium* and *Bacteroides* were significantly decreased in mothers consuming the iron-deficient diet, with a corresponding reduction in the relative amounts of these bacteria in their offspring. Compared with the LI and NI groups, the N,O-CMCS-iron consumption markedly enhanced the relative abundances of Bacteroidetes, Bacteroidaceae and *Butyricimonas* of the pregnant and lactating dams. In addition, the N,O-CMCS-iron supplementation increased the relative abundance of *Clostridium* in the lactating dams. Since most gut bacteria need iron to survive, the amount of iron present in the gastrointestinal tract may have an impact on bacteria thriving in that environment. Consistent with our results, Bacteroidetes species and *Clostridium* were greatly reduced in iron deficiency models from other studies[55,56]. Importantly, the amounts of Bacteroidetes, Bacteroidaceae, *Butyricimonas and Clostridium* in the offspring mice of the CI group were also significantly higher than those of the other two groups. The gut ecosystem is established at or soon after birth and is enhanced by vertical transmission, ingestion of or exposure to environmental microbiota[57]. Thus, the concordance between maternal and offspring microbiome profiles likely reflects mother-to-infant microbial transfer. Moreover, we were very surprised to find that when all groups of the weaned offspring mice were equally fed ferrous sulfate in the Exp. 2, the contents of Bacteroidetes, Bacteroidaceae*, Butyricimonas and Clostridium* in the offspring mice from the CI group were still significantly enhanced relative to mice from the

LI and NI groups. These results underscored the long-term influence of maternal nutritional status on the intestinal flora composition of their offspring.

It is noteworthy that we observed almost no remarkable changes in the gut microbiota composition between the LI and NI dams, or between their offspring. Actually there are conflicting findings regarding the relationship between ferrous sulfate as an iron supplement and gut microbiota. Dostal et al.[58] demonstrated that repletion with ferrous sulfate diet could partially restore bacterial populations compared to iron-deficient rats. But in line with our findings, an earlier investigation also reported no significant changes in microbial communities in mice treated with ferrous sulfate following iron deficiency[59]. Another study even discovered that giving ferrous sulfate to infants with adequate iron levels had negative impacts on their gut microbiome, leading to higher concentrations of pathogenic bacteria[53]. One of the undeniable advantages of using polysaccharide-iron as an iron supplement lies in polysaccharides can also be absorbed by the body and play a prebiotic role. Earlier studies have widely reported that dietary supplementation with chitosan or its derivatives greatly increased the relative abundances of beneficial bacteria, such as *Bacteroides, Prevotella* and so on[60,61]. A former reasearch revealed that carboxymethyl chitosan exerts superior modulatory effects on gut flora both in vitro and in vivo[62]. Our study also demonstrated that the N,O-CMCS complex positively regulated the gut microbiota in mice, suggesting that it is a promising alternative to ferrous salts for managing iron deficiency. The complexation of polysaccharides with trace element ions actually can create a synergistic effect, enhancing the original biological activities of both components.

SCFAs are produced by intestinal microbiota which metabolizes prebiotics, and the supply of appropriate and sufficient dietary fiber modulates bacteria composition and SCFAs production in the gut. Through functional annotation of the metagenomic KEGG database in the Exp. 2, we found significant enrichment of fatty acid biosynthesis pathways in the CI group offspring. There are four different routes for butyrate synthesis: the Acetyl-CoA pathway, the Lysine pathway, the Glutarate pathway, and the 4-Aminobutyrate pathway, among which the Acetyl-CoA pathway is the most common butyrate-producing pathway. Dietary carbohydrates are mainly digested and absorbed in the colon, where ATP is produced through the substrate phosphorylation and then utilized by butyrate producers. In this process, carbohydrates are metabolized to create intermediates such as pyruvate, acetyl coenzyme A, etc. The transition from crotonyl-CoA to butyryl-CoA is the central step of the Acetyl-CoA pathway, which is also shared by the other three pathways. The last step from butyryl-CoA to butyrate is catalyzed either by butyryl-CoA:acetate CoA transferase (encoded by *but*), or by phosphate butyryltransferase and butyrate kinase (encoded by *buk*). These genes are typically used as indicators to identify butyrate-producing communities[63]. In our study, the contents of genes encoding phosphate butyryltransferase and butyrate kinase were both remarkably elevated in the offspring mice of dams that ingested N,O-CMCS-iron. Our findings revealed that the addition of N,O-CMCS-iron to the maternal diet markedly improved the butyrate-producing capacity of the gut microbes of their offspring. Indeed, in agreement with changes in the metagomic KEGG functional annotation, we found that the colonic butyrate level was significantly higher in CI dams and their offspring

compared to other dietary groups. Correlation analysis revealed significant positive associations between the butyrate content and the relative abundances of Clostridiaceae, *Clostridium* and *Butyricimonas*. *Butyricimonas* is a known butyrate-producer whose content is significantly reduced in many pathological conditions[64]. Clostridiaceae and its members including *Clostridium* have the capacity of consuming undigested dietary fibers and synthesizing SCFAs, particularly acetate and butyrate[65]. These results further confirmed the effect of microbial transmission between mothers and their offspring.

As key mediators of the gut-brain axis, the gut microbiota is critical for cognitive performance, and SCFAs are generally regarded as pivotal candidate mediators driving this communication..Due to their neuroactive characteristics and impacts on other gut-brain signaling pathways, SCFAs may be involved in communication along the microbiota-gut-brain axis either directly or indirectly[66]. SCFAs can pass cross the blood-brain barrier (BBB) and enter the brain, and an animal study showed that the proportion of SCFAs ingested through the BBB in the rat brain was in the relative order of butyrate (the highest), propionate, and acetate[67]. The content of SCFAs, especially butyrate, may be decisive in deciding its impact on behavioral and psychophysiological processes. A study demonstrated that administration of butyrate significantly counteracted cognitive impairment and neural morphology induced by quinolinic acid in rodents models that relevant to obesity, indicating the beneficial effect of butyrate on alleviating neurodegeneration[68]. In the Morris water maze test, butyrate has been shown to ameliorate memory impairment and anxiety symptoms in lead-exposed mice, as evidenced by the reduced escape latency and the increased frequency of platform crossings. Moreover, butyrate restored the protein level of neurotrophic factors such as BDNF[69]. Therefore, we proposed that maternal N,O-CMCS-iron supplementation increased the abundance of butyrate-producing bacteria in dams and their offspring, and that the elevated butyrate content ultimately improved the cognitive function in the offspring mice via the gut-brain axis.

To further explore the possible mechanism by which N,O-CMCS-iron more significantly enhanced the brain function in mice, we attempted to identify the differentially expressed pathways in the offspring through RNA sequencing. Compared with the LI and NI groups, the HIF-1α signaling pathway was markedly enriched in the offsping mice from the CI group. HIF-1α is a ubiquitously expressed transcription factor that regulates the transcription of genes implicated in a wide range of physiological procedures including angiogenesis, erythropoiesis, iron homeostasis, glucose metabolism, anti-inflammation, antioxidation, etc[70]. These adaptive response processes mediated by HIF-1α signaling are closely related to its neuroprotective effect. Studies have confirmed that the use of HIF-1α agonist improved cognitive impairment in patients with Alzheimer's disease (AD)[31]. HIF-1α also diminished nerve cell death caused by oxidative stress and attenuated hippocampal neuronal apoptosis induced by Aβ[71]. A study reported that up-regulating HIF-1α expression effectively reduced the cerebral infarction volume and promoted the recovery of motor function in rats, which was connected to the activation of the downstream target gene VEGF of HIF-1α[72]. The neuroprotective role of VEGF mainly lies in its ability to enhance the proliferation of endothelial cells and the generation of blood vessels, and improve the local blood circulation of the brain[73]. Furthermore, VEGF has a

direct protective effect on neural tissue. In vitro culture, VEGF significantly increased the survival rate of neurons in serum-free or other harmful environments[73,74]. In our study, the expression levels of several downstream genes involved in angiogenesis in the HIF-1α signaling such as *Vegfa*, *Angpt2* and *Flt1* were indeed elevated under N,O-CMCS-iron treatment. Glucose is a key source of energy for mammalian brain tissue and maintains the normal function of neurons. Insufficient glucose supply is a hallmark of brain aging and is particularly prominent in neurodegenerative diseases like AD[75]. GLUT1 (encoded by *Scl21a1*) is engaged in the regulation of glucose transport and maintenance of the BBB. A reduction in the quantity or functional abnormality of GLUT1 will lead to disorders of glucose metabolism in the brain. Researches have shown that the content of GLUT1 was reduced in the brain tissues of AD patients and rodent AD models. Furthermore, GLUT1 deficiency in the endocortex of mice with overexpression of Aβ lead to BBB disruption and related cerebrovascular degenerative changes, and progressive neuronal degeneration[76]. In this study, the downstream genes engaged in glycolysis in the HIF-1α signaling including *Scl21a1*, *Aldob* and *Eno3* were enriched in the CI group, suggesting that the administration of N,O-CMCS-iron improved glucose metabolism and energy supply in the brain. In addition, we also observed that the transcription of iron metabolism gene *Tfrc* was increased in the CI group. Iron chelators upregulating HIF-1α have been shown to differentially induce TFRC across brain regions in adult mice[77]. And there are studies demonstrated that the HIF-prolylhydroxylase inhibitor Roxadustat could improve iron metabolism[78,79]. Within brain cells, TFRC has been found in neurons, capillary endothelial cells, and choroidal plexus epithelial cells[80]. Iron uptake in the brain is a highly regulated process, which requires iron be translocated across the BBB into the central nervous system, and the interaction between TF and TFRC appears to play this role in the BBB. A prevailing view is that TF-Fe complexes are uptaken into the brain interstitial fluid via receptor-mediated endocytosis of the TFRC. One study showed that pretreatment of rodents with a monoclonal antibody against TFRC suppressed iron transport to the brain by 35%-85%[81]. The above evidence confirms that the HIF-1α signaling pathway and its downstream gene, *Tfrc*, play an important role in enhancing iron uptake in the brain. Our experimental results indicated that the offspring mice from N,O-CMCS-iron-supplemented dams still had significantly higher brain cognitive function than other mice even after weaning when they consume the same diet as other mice. This may be attributed to the ability of N,O-CMCS-iron to robustly activate HIF-1α signaling, promoting angiogenesis, glucose metabolism and iron homeostasis in the brain, thereby exerting neuroprotective effects. We did not detect the expression of HIF-1α itself, which may be due to the fact that HIF-1α expression has a transient induction effect and is susceptible to degradation, making it difficult to accurately capture its expression moment. However, both RT-qPCR and western bolt analysis demonstrated that the levels of other downstream genes of HIF-1α such as *Slc2a1*, *Eno3* and so on were also significantly elevated in the brains of the CI offspring mice, confirming the enrichment of HIF-1α signaling under N,O-CMCS-iron treatment.

Notably, several reports have linked the butyrate function to HIF-1α stabilization. One study showed that sodium butyrate treatment greatly enhanced the nuclear HIF-1α and promoted barrier function in Caco2 cells.

In addition, they found that antibiotic-mediated microbiota consumption decreased colonic butyrate and HIF expression, both of which were restored by butyrate supplementation[82]. Another study proved that HIF-1α signaling was necessary for the protective effect of butyrate on the intestinal epithelium, since they observed that oral delivery of butyrate promoted the contents of colonic HIF-1α mRNA and its target genes in mice infected with *Clostridium difficile,* and the effect was relevant to the intestinal barrier integrity[83]. These results highlight that butyrate exerts its intestinal protective effect through a HIF-1α-dependent mechanism. In this study, we revealed that the butyrate level was positively correlated with the contents of HIF-1α downstream target genes in the brain. Moreover, we conducted an in vitro cell experiment using the mouse hippocampal neuron cell line HT-22. The results demonstrated that the butyrate treatment indeed enhanced the protein expression of HIF-1α and its downstream proteins such as TFRC and GLUT1 in HT-22 cells. Therefore, it can be reasonably concluded that maternal N,O-CMCS-iron intake increased butyrate-producing microbe abundance and butyrate production in both dams and their offspring, and that the enhanced butyrate stabilized HIF-1α signaling in the brain after crossing the BBB, which promoted the iron absorption in brain and ultimately improved the cognitive function in the offspring. While current evidence linking butyrate and HIF-1α primarily originates from intestinal studies, our data provide novel insights into its role in the brain. Substantial evidence supports a positive association between butyrate-producing bacteria and brain health. One previous study reported that *Butyricimonas* was capable of improving the neurological function in a stroke animal model[79]. Another study also identified *Butyricimonas* as one of the cognition-related genera, which was depleted in cognitively impaired participants compared to normal controls[84]. In addition, Clostridiaceae performs a protective role in gut health, and its decline has been linked to reduced intrinsic brain activity and cognitive performance[85], indicating that it could be a biomarker in forecasting the brain development. And within the Clostridiaceae family, *Clostridium* typically had an increased relative abundance in patients with better brain function[86].

The present study has several strengths worth mentioning. First of all, we synthesized a new type of polysaccharide-iron with a higher iron content, namely the N,O-CMCS-iron complex. Secondly, we have demonstrated that compared to inorganic iron, maternal intake of the N,O-CMCS-iron complex could improve the gut microbiota composition and metabolism of the offspring mice through vertical transmission effects, and further enhance the cognitive function of the offspring mice through the gut-brain communicaiton. Finally, we revealed the positive regulatory effect of butyrate on the HIF-1α signaling pathway in the brain through correlation analysis and in vitro experiments, which provides a new perspective for understanding the role of butyrate and the HIF-1α signaling in promoting brain cognition. However, some limitations must also be considered when interpreting the results of this study. On the one hand, although we have revealed that the offspring mice showing the same consistency with the maternal gut microbiome changes owing to a mother-to-child transmission effect, we didn’t perform the strain-level tracing. Our microbiome analysis results have identified that both the mothers that consumed the N,O-CMCS-iron complex and their offspring mice showed the increased levels of beneficial microorganisms such as Clostridiaceae, *Butyricimonas* and

Clostridium. Future investigation can further explore the specific strains that exert beneficial effects at the species level, in order to guide deeper mechanism research and exploration of applications. On the other hand, the end point of this study was set at the 42nd day after the birth of mice. To further clarify the long-term effect of the N,O-CMCS-iron complex on improving cognitive function, the follow-up period for mice after weaning could be extended in future studies.

5. Conclusion

In a word, we successfully synthesized and characterized the N,O-CMCS-iron complex, and our mouse model exhibited that ingestion of N,O-CMCS-iron by mothers during pregnancy and lactation distinctly improved the brain cognitive ability in the offspring mice. We found that maternal intake of N,O-CMCS-iron could not only markedly increase the iron storage in offspring, but also promoted the gut microbiota composition and elevated the butyrate level in both dams and their offspring. And importantly, we further revealed that the increase of microbial-derived butyrate might potentiate the HIF-1α signaling pathway and its downstream target genes in the brain of offspring, thereby improved the brain microenvironment by regulating the physiological procedures including angiogenesis, glucose metabolism and iron uptake in the brain, and ultimately strengthened the cognitive cognition of the offspring mice. Our study provides data to support the development of N,O-CMCS-iron as a novel iron supplement to enhance the brain cognitive function. This is of great significance for the further exploitation of other new polysaccharide-iron complex. Meanwhile, it provides new ideas for in-depth research on the mechanism by which polysaccharide-iron promotes brain cognition through enhancing gut-brain communication, and helps to further identify molecular targets that can improve brain function.

Declaration of competing interest

The authors declare no conflict of interest.

Acknowledgments

This study was supported by the Young Scientists Fund of the National Natural Science Foundation of China (32302752) and Key Research and Development Program of Shaanxi (2022QCY-LL-52).

Data availability

Data will be made available on request.

References

[1] S.R. Pasricha, J. Tye-Din, M.U. Muckenthaler, et al., Iron deficiency, Lancet 397 (2021) 233-248. https://doi.org/10.1016/S0140-6736(20)32594-0.

[2] M.K. Georgieff, Iron deficiency in pregnancy, Am. J. Obstet. Gynecol. 223 (2020) 516-524. https://doi.org/10.1016/j.ajog.2020.03.006.

[3] K.L. Lindsay, C. Buss, P.D. Wadhwa, et al., The interplay between nutrition and stress in pregnancy: Implications for fetal programming of brain development, Biol. Psychiatry 85 (2019) 135-149. https://doi.org/10.1016/j.biopsych.2018.06.021.

[4] M. Egbor, T. Ansari, N. Morris, et al., Morphometric placental villous and vascular abnormalities in early- and late-onset pre-eclampsia with and without fetal growth restriction, BJOG 113 (2006) 580-589. https://doi.org/10.1111/j.1471-0528.2006.00882.x.

[5] S. Faruk, K.O. Sanusi, K.G. Ibrahim, et al., Age and sex-based impacts of maternal iron deficiency on offspring's cognitive function and anemia: A systematic review, Eur. J. Clin. Nutr. 78 (2024) 477-485. https://doi.org/10.1038/s41430-024-01423-x.

[6] E.L. Unger, A.R. Hurst, M.K. Georgieff, et al., Behavior and monoamine deficits in prenatal and perinatal iron deficiency are not corrected by early postnatal moderate-iron or high-iron diets in rats, J. Nutr. 142 (2012) 2040-2049. https://doi.org/10.3945/jn.112.162198.

[7] C. Camaschella, Iron-deficiency anemia, N. Engl. J. Med. 372 (2015) 1832-1843. https://doi.org/10.1056/NEJMra1401038.

[8] X. Yan, Q. Zhang, T. Wang, et al., Evaluation of different polysaccharide-iron complex preparations in vitro and in vivo, Pharmaceutics 17 (2025) 292. https://doi.org/10.3390/pharmaceutics17030292.

[9] Y. Feng, Y. Wu, J. Wang, et al., Enteromorpha prolifera polysaccharide-Fe (III) complex promotes intestinal development as a new iron supplement, Sci. China Life Sci. 68 (2025) 219-231. https://doi.org/10.1007/s11427-023-2562-9.

[10] B. Graczykowski, A. Dobek, Iron-dextran complex: Geometrical structure and magneto-optical features, J. Colloid Interface Sci. 363 (2011) 551-556. https://doi.org/10.1016/j.jcis.2011.07.080.

[11] J.C. Montano-Pedroso, E.B. Garcia, M.A.R. de Moraes, et al., Intravenous iron sucrose versus oral iron administration for the postoperative treatment of post-bariatric abdominoplasty anaemia: an open-label, randomised, superiority trial in Brazil, Lancet Haematol. 5 (2018) e310-e320. https://doi.org/10.1016/S2352-3026(18)30071-1.

[12] N.K. Das, A.J. Schwartz, G. Barthel, et al., Microbial metabolite signaling is required for systemic iron homeostasis, Cell Metab. 31 (2020) 115-130. https://doi.org/10.1016/j.cmet.2019.10.005.

[13] B. Qi, M. Han, Microbial siderophore enterobactin promotes mitochondrial iron uptake and development of the host via interaction with ATP synthase, Cell 175 (2018) 571-582. https://doi.org/10.1016/j.cell.2018.07.032.

[14] M. Rosell-Díaz, E. Santos-González, A. Motger-Albertí, et al., Gut microbiota links to serum ferritin and cognition, Gut Microbes 15 (2023) 2290318. https://doi.org/10.1080/19490976.2023.2290318.

[15] Z.H. Almahal, A. Hasan, S.A. Razzak, et al., Molecular perspective of dietary influences on the gut microbiome alongside neurological health: Exploring the gut-brain axis, ACS Chem. Neurosci. 16 (2025) 1996-2012. https://doi.org/10.1021/acschemneuro.5c00058.

[16] A. Zipperer, M.C. Konnerth, C. Laux, et al., Human commensals producing a novel antibiotic impair pathogen colonization, Nature 535 (2016) 511-516. https://doi.org/10.1038/nature18634.

[17] A.S. Wadan, M.K.A. El-Aziz, D.E. Ellakwa, The microbiota-gut-brain-axis theory: role of gut microbiota modulators (GMMs) in gastrointestinal, neurological, and mental health disorders, Naunyn Schmiedebergs Arch. Pharmacol. 398 (2025) 13397-13426. https://doi.org/10.1007/s00210-025-04155-2.

[18] P. Ferretti, E. Pasolli, A. Tett, et al., Mother-to-infant microbial transmission from different body sites shapes the developing infant gut microbiome, Cell Host & Microbe 24 (2018) 133-145. https://doi.org/10.1016/j.chom.2018.06.005.

[19] S.A. Buffington, G.V. Di Prisco, T.A. Auchtung, et al., Microbial reconstitution reverses maternal diet-induced social and synaptic deficits in offspring, Cell 165 (2016) 1762-1775. https://doi.org/10.1016/j.cell.2016.06.001.

[20] J. Zou, V.L. Ngo, Y. Wang, et al., Maternal fiber deprivation alters microbiota in offspring, resulting in low-grade inflammation and predisposition to obesity, Cell Host & Microbe 31 (2023) 45-57. https://doi.org/10.1016/j.chom.2022.10.014.

[21] G. He, B. Zhang, T. Chen, et al., Effects of chitosan on restoring spermatogenesis in mice: Insights from gut microbiota and multi-omics analysis, Food Res. Int. 208 (2025) 116218. https://doi.org/10.1016/j.foodres.2025.116218.

[22] X. Wu, M.J. Kim, H.J. Yang, et al., Chitosan alleviated menopausal symptoms and modulated the gut microbiota in estrogen-deficient rats, Eur. J. Nutr. 60 (2021) 1907-1919. https://doi.org/10.1007/s00394-020-02382-2.

[23] L. Zhu, B. Hu, Y. Guo, et al., Effect of Chitosan oligosaccharides on ischemic symptom and gut microbiota disbalance in mice with hindlimb ischemia, Carbohydr. Polym. 240 (2020) 116271. https://doi.org/10.1016/j.carbpol.2020.116271.

[24] H. Cao, J. He, Emerging roles and advanced applications of carboxymethyl chitosan in food technology: A review, Food Hydrocolloids 280 (2025) 111197. https://doi.org/10.1016/j.foodhyd.2025.111197.

[25] J. Yang, The preparation of N, N'-dicarboxymethyl chitosan-iron complex and experimental studies of cure iron-deficiency anemia (in Chinese). Shandong: Qingdao University of Science and Technology. (2011)

[26] L. García, S. Braccini, E. Pagliarini, et al., Ionically-crosslinked carboxymethyl chitosan scaffolds by additive manufacturing for antimicrobial wound dressing applications, Carbohydr. Polym. 346 (2024) 122640. https://doi.org/10.1016/j.carbpol.2024.122640.

[27] K. Loukelis, V. Tsampallas, M. Kaliva, et al., Synthesis of N, N,O and O-carboxymethyl chitosan derivatives of controllable substitution degrees and their utilization as electrospun scaffolds for bone tissue engineering, Carbohydr. Polym. 348 (2024) 122775. https://doi.org/10.1016/j.carbpol.2024.122775.

[28] P. Liu, M. Zhang, T. Liu, et al., Avenanthramide improves colonic damage induced by food allergies in mice through altering gut microbiota and regulating Hsp70-NF-κB signaling, Nutrients 15 (2023) 992. https://doi.org/10.3390/nu15040992.

[29] R. Liu, X. Xiao, J. Gong, et al., Genetic linkage analysis of stable QTLs in Gossypium hirsutum RIL population revealed function of GhCesA4 in fiber development, J. Adv. Res. 65 (2024) 33-46. https://doi.org/10.1016/j.jare.2023.12.005.

[30] E. Schneider, K.J. O'Riordan, G. Clarke, et al., Feeding gut microbes to nourish the brain: unravelling the diet-microbiota-gut-brain axis, Nat. Metab. 6 (2024) 1454-1478. https://doi.org/10.1038/s42255-024-01108-6.

[31] R.D. Bell, B.V. Zlokovic, Neurovascular mechanisms and blood-brain barrier disorder in Alzheimer's disease, Acta Neuropathol. 118 (2009) 103-113. https://doi.org/10.1007/s00401-009-0522-3.

[32] J. Beard, K.M. Erikson, B.C. Jones, Neonatal iron deficiency results in irreversible changes in dopamine function in rats, J. Nutr. 133 (2003) 1174-1179. https://doi.org/10.1093/jn/133.4.1174.

[33] A.F. Lukowski, M. Koss, M.J. Burden, et al., Iron deficiency in infancy and neurocognitive functioning at 19 years: evidence of long-term deficits in executive function and recognition memory, Nutr. Neurosci. 13 (2010) 54-70. https://doi.org/10.1179/147683010X12611460763689.

[34] X. Zhu, P. Yuan, T. Zhang, et al., Effect of carboxymethyl chitosan on the storage stability of frozen dough: State of water, protein structures and quality attributes, Food Res. Int. 151 (2022) 110863. https://doi.org/10.1016/j.foodres.2021.110863.

[35] Z. Shariatinia, Carboxymethyl chitosan: Properties and biomedical applications, Int. J. Biol. Macromol. 120 (2018) 1406-1419. https://doi.org/10.1016/j.ijbiomac.2018.09.131.

[36] J. Kim, M. Wessling-Resnick, Iron and mechanisms of emotional behavior, J. Nutr. Biochem. 25 (2014) 1101-1107. https://doi.org/10.1016/j.jnutbio.2014.07.003.

[37] T. Tufail, H.B.U. Ain, M.S. Virk, et al., GABA (γ-aminobutyric acid) enrichment and detection methods in cereals: Unlocking sustainable health benefits, Food Chem. 464 (2025) 141750. https://doi.org/10.1016/j.foodchem.2024.141750.

[38] M. Kaladhar, B.N. Rao, Effect of maternal iron deficiency in rat on serotonin uptake in vitro by brain synaptic vesicles in the offspring, J. Neurochem. 40 (1983) 1768-1770. https://doi.org/10.1111/j.1471-4159.1983.tb08155.x.

[39] P.V. Tran, S.J. Fretham, E.S. Carlson, et al., Long-term reduction of hippocampal brain-derived neurotrophic factor activity after fetal-neonatal iron deficiency in adult rats, Pediatr. Res. 65 (2009) 493-498. https://doi.org/10.1203/PDR.0b013e31819d90a1.

[40] B. Liu, W. Xin, J.R. Tan, et al., Myelin sheath structure and regeneration in peripheral nerve injury repair, Proc. Natl. Acad. Sci. U.S.A 116 (2019) 22347-22352. https://doi.org/10.1073/pnas.1910292116.

[41] R.M. Amos-Kroohs, V. Usach, G. Piñero, et al., Metal bashing: Iron deficiency and manganese overexposure impact on peripheral nerves, J. Toxicol. Environ. Health A. 82 (2019) 99-112. https://doi.org/10.1080/15287394.2019.1566105.

[42] L.A. Jorgenson, J.D. Wobken, M.K. Georgieff, Perinatal iron deficiency alters apical dendritic growth in hippocampal CA1 pyramidal neurons, Dev. Neurosci. 25 (2004) 412-420. https://doi.org/10.1159/000075667.

[43] B. Lozoff, E. Jimenez, J. Hagen, et al., Poorer behavioral and developmental outcome more than 10 years after treatment for iron deficiency in infancy, Pediatrics 105 (2000) E51. https://doi.org/10.1542/peds.105.4.e51.

[44] P. Peirano, C. Algarin, M. Garrido, et al., Cerebral executive function in preadolescents is affected by iron deficiency in infancy, Pediatr. Res. 55 (2004) 279A.

[45] M. Burden, M. Koss, B. Lozoff, et al., Neurocognitive differences in 19-year-olds treated for iron deficiency in infancy, Pediatr. Res. 55 (2004) 279A.

[46] J.L. Beard, B. Felt, T. Schallert, et al., Moderate iron deficiency in infancy: Biology and behavior in young rats, Behav. Brain Res. 170 (2006) 224-232. https://doi.org/10.1016/j.bbr.2006.02.024.

[47] B.T. Felt, J.L. Beard, T. Schallert, et al., Persistent neurochemical and behavioral abnormalities in adulthood despite early iron supplementation for perinatal iron deficiency anemia in rats, Brain Behav. Res. 171 (2006) 261-270. https://doi.org/10.1016/j.bbr.2006.04.001.

[48] E. Findlay, K.T. Ng, R.L. Reid, et al., The effect of iron deficiency during development on passive avoidance learning in the adult rat, Physiol. Behav. 27 (1981) 1089-1096. https://doi.org/10.1016/0031-9384(81)90375-9.

[49] J-L. Jougleux, F.M. Rioux, M.W. Church, et al., Dietary LCPUFA in iron-deficient anaemic pregnant and lactating guinea pigs induce minor defects in the offsprings' auditory brainstem responses, Nutr. Neurosci. 19 (2016) 447-460. https://doi.org/10.1179/1476830514Y.0000000140.

[50] P. Boksa, Y. Zhang, D. Nouel, et al., Early development of Parvalbumin-, somatostatin-, and cholecystokinin-expressing neurons in rat brain following prenatal immune activation and maternal iron deficiency, Dev. Neurosci. 38 (2016) 342-353. https://doi.org/10.1159/000454677.

[51] V. Sangkhae, A.L. Fisher, S. Wong, et al., Effects of maternal iron status on placental and fetal iron homeostasis, J. Clin. Investig. 130 (2021) 625-640. https://doi.org/10.1172/JCI127341.

[52] R. Eseh, B. Zimmerberg. Age-dependent effects of gestational and lactational iron deficiency on anxiety behavior in rats, Behav. Brain Res. 164 (2005) 214-221. https://doi.org/10.1016/j.bbr.2005.06.019.

[53] K.S. Sjödin, M. Domellöf, C. Lagerqvist, et al., Administration of ferrous sulfate drops has significant effects on the gut microbiota of iron-sufficient infants: a randomised controlled study, Gut 68 (2019) 2095-2097. https://doi.org/10.1136/gutjnl-2018-316988.

[54] J. Han, J. Xiong, Z. Bai, et al., Tuna dark muscle peptides modulate host iron metabolism in the intestine through the gut microbiota and ameliorate iron deficiency anemia, Food Sci. Hum. Well 14 (2025) 9250047. http://doi.org/10.26599/FSHW.2024.9250047.

[55] L.C. Knight, M. Wang, S.M. Donovan, et al., Early-life iron deficiency and subsequent repletion alters development of the colonic microbiota in the pig, Front. Nutr. 6 (2019) 120. https://doi.org/10.3389/fnut.2019.00120.

[56] T. Jaeggi, G.A. Kortman, D. Moretti, et al., Iron fortification adversely affects the gut microbiome, increases pathogen abundance and induces intestinal inflammation in Kenyan infants, Gut 64 (2015) 731-742. https://doi.org/10.1136/gutjnl-2014-307720.

[57] E. Bradley, J. Haran, The human gut microbiome and aging, Gut Microbes 16 (2024) 2359677. https://doi.org/10.1080/19490976.2024.2359677.

[58] A. Dostal, C. Chassard, F.M. Hilty, et al., Iron depletion and repletion with ferrous sulfate or electrolytic iron modifies the composition and metabolic activity of the gut microbiota in rats, J. Nutr. 142 (2012) 271-277. https://doi.org/10.3945/jn.111.148643.

[59] M. Zakrzewski, S.J. Wilkins, S.L. Helman, et al., Supplementation with Sucrosomial® iron leads to favourable changes in the intestinal microbiome when compared to ferrous sulfate in mice, Biometals 35 (2022) 27-38. https://doi.org/10.1007/s10534-021-00348-3.

[60] T. Yu, Y. Wang, S. Chen, et al., Low-molecular-weight chitosan supplementation increases the population of Prevotella in the cecal contents of weanling pigs, Front. Microbiol. 8 (2017) 2182. https://doi.org/10.3389/fmicb.2017.02182.

[61] J. Zheng, X. Yuan, G. Cheng, et al., Chitosan oligosaccharides improve the disturbance in glucose metabolism and reverse the dysbiosis of gut microbiota in diabetic mice, Carbohydr. Polym. 190 (2018) 77-86. https://doi.org/10.1016/j.carbpol.2018.02.058.

[62] X. Pan, P. Liu, Y. Zhang, et al., Carboxymethyl chitosan-TK resistant starch complex ameliorates type 2 diabetes by regulating the gut microbiota, Int. J. Biol. Macromol. 253 (2023) 126930. https://doi.org/10.1016/j.ijbiomac.2023.126930.

[63] M. Vital, A.C. Howe, J.M. Tiedje, Revealing the bacterial butyrate synthesis pathways by analyzing (meta)genomic data, mBio 5 (2014) e00889. https://doi.org/10.1128/mBio.00889-14.

[64] N.D. Nuzum, E.A. Szymlek-Gay, S. Loke, et al., Differences in the gut microbiome across typical ageing and in Parkinson's disease, Neuropharmacology 235 (2023) 109566. https://doi.org/10.1016/j.neuropharm.2023.109566.

[65] M.K. Stoeva, J. Garcia-So, N. Justice, et al., Butyrate-producing human gut symbiont, Clostridium butyricum, and its role in health and disease, Gut Microbes 13 (2021) 1907272. https://doi.org/10.1080/19490976.2021.1907272.

[66] B. Dalile, L. Van Oudenhove, B. Vervliet, et al., The role of short-chain fatty acids in microbiota-gut-brain communication, Nat. Rev. Gastroenterol. Hepatol. 16 (2019) 461-478. https://doi.org/10.1038/s41575-019-0157-3.

[67] W.H. Oldendorf, Carrier-mediated blood-brain barrier transport of short-chain monocarboxylic organic acids, Am. J. Physiol. 224 (1973) 1450-1453. https://doi.org/10.1152/ajplegacy.1973.224.6.1450.

[68] X. Ge, M. Zheng, M. Hu, et al., Butyrate ameliorates quinolinic acid-induced cognitive decline in obesity models, J. Clin. Invest. 133 (2023) e154612. https://doi.org/10.1172/JCI154612.

[69] Y. Li, A. Liu, K. Chen, et al., Sodium butyrate alleviates lead-induced neuroinflammation and improves cognitive and memory impairment through the ACSS2/H3K9ac/BDNF pathway, Environ. Int. 184 (2024) 108479. https://doi.org/10.1016/j.envint.2024.108479.

[70] X. Huang, Y. Zhang, B. Qi, et al., HIF-1α: Its notable role in the maintenance of oxygen, bone and iron homeostasis (Review), Int. J. Mol. Med. 50 (2022) 141. https://doi.org/10.3892/ijmm.2022.5197.

[71] E.V. Mitroshina, M.O. Savyuk, E. Ponimaskin, et al., Hypoxia-inducible factor (HIF) in ischemic stroke and neurodegenerative disease, Front. Cell. Dev. Biol. 9 (2023) 703084. https://doi.org/10.3389/fcell.2021.703084.

[72] S. Nagel, M. Papadakis, R. Chen, et al., Neuroprotection by dimethyloxalylglycine following permanent and transient focal cerebral ischemia in rats, J. Cereb. Blood Flow Metab. 31 (2011) 132-143. https://doi.org/10.1038/jcbfm.2010.60.

[73] D.A. Greenberg, K. Jin, Vascular endothelial growth factors (VEGFs) and stroke, Cell Mol. Life Sci. 70 (2013) 1753-1761. https://doi.org/10.1007/s00018-013-1282-8.

[74] Y. Ma, W. Liu, Y. Wang, et al., VEGF protects rat cortical neurons from mechanical trauma injury induced apoptosis via the MEK/ERK pathway, Brain Res. Bull. 86 (2011) 441-446. https://doi.org/10.1016/j.brainresbull.2011.07.007.

[75] A. Xu, Y. Tang, Q. Zeng, et al., Electroacupuncture Enhances Cognition by Promoting Brain Glucose Metabolism and Inhibiting Inflammation in the APP/PS1 Mouse Model of Alzheimer's Disease: A Pilot Study, J. Alzheimers. Dis. 77 (2020) 387-400. https://doi.org/10.3233/JAD-200242.

[76] X.J. Xu, M.S. Yang, B. Zhang, et al., Glucose metabolism: A link between traumatic brain injury and Alzheimer's disease, Chin. J. Traumatol. 24 (2021) 5-10. https://doi.org/10.1016/j.cjtee.2020.10.001.

[77] J. Lim, H.I. Kim, Y. Bang, et al., Hypoxia-inducible factor-1α upregulates tyrosine hydroxylase and dopamine transporter by nuclear receptor ERRγ in SH-SY5Y cells, Neuroreport 26 (2015) 380-386. https://doi.org/10.1097/WNR.0000000000000356.

[78] Y. Ikeda, Novel roles of HIF-PHIs in chronic kidney disease: the link between iron metabolism, Kidney Int. 100 (2021) 14-16. https://doi.org/10.1016/j.kint.2021.04.030.

[79] N. Chen, C. Hao, X. Peng, et al., Roxadustat for anemia in patients with kidney disease not receiving dialysis, N. Engl. J. Med. 381 (2019) 1001-1010. https://doi.org/10.1056/NEJMoa1813599.

[80] T. Moos, E.H. Morgan, Transferrin and transferrin receptor function in brain barrier systems, Cell Mol. Neurobiol. 20 (2000) 77-95. https://doi.org/10.1023/a:1006948027674.

[81] F.R.K.B. Ueda, K.B. Raja, R.J. Simpson, et al., Rate of 59Fe uptake into brain and cerebrospinal fluid and the influence thereon of antibodies against the transferrin receptor, J. Neurochem. 60 (1993) 106-113. https://doi.org/10.1111/j.1471-4159.1993.tb05828.x.

[82] C.J. Kelly, L. Zheng, E.L. Campbell, et al., Crosstalk between microbiota-derived short-chain fatty acids and intestinal epithelial HIF augments tissue barrier function, Cell Host & Microbe 17 (2015) 662-671. https://doi.org/10.1016/j.chom.2015.03.005.

[83] J.L. Fachi, J. de Souza Felipe, L.P. Pral, et al., Butyrate protects mice from Clostridium difficile-induced colitis through an HIF-1-dependent mechanism, Cell Rep. 27 (2019) 750-761. https://doi.org/10.1016/j.celrep.2019.03.054.

[84] X. Liang, Y. Fu, W.T. Cao, et al., Gut microbiome, cognitive function and brain structure: a multi-omics integration analysis, Transl. Neurodegener. 11 (2022) 49. https://doi.org/10.1186/s40035-022-00323-z.

[85] P. Liu, X.Z. Jia, Y. Chen, et al., Gut microbiota interacts with intrinsic brain activity of patients with amnestic mild cognitive impairment, CNS Neurosci. Ther. 27 (2021) 163-173. https://doi.org/10.1111/cns.13451.

[86] J.S. Bajaj, A. Fagan, M.B. White, et al., Specific gut and salivary microbiota patterns are linked with different cognitive testing strategies in minimal hepatic encephalopathy, Am. J. Gastroenterol. 114 (2019) 1080-1090. https://doi.org/10.14309/ajg.0000000000000102.